Available online at www.sciencedirect.com
ScienceDirect
Renewable and Sustainable Energy Reviews
12 (2008) 1485–1528
RENEWABLE & SUSTAINABLE ENERGY REVIEWS
www.elsevier.com/locate/rser

A review of the mathematical models for predicting rotary desiccant wheel

T.S. Ge, Y. Li, R.Z. Wang*, Y.J. Dai

Institute of Refrigeration and Cryogenics, Shanghai Jiao Tong University, Shanghai 200240, PR China

Received 6 November 2006; accepted 22 January 2007

Abstract

In the solid desiccant wheel air-conditioning system, the performance of the desiccant wheel is critical to the capability, size and cost of the whole system. Constructing mathematical model is an effective method for analyzing the performance of the rotary wheel as well as the system. The model can also be used to guide system operation, interpret experimental results and assist in system design and optimization. The overall objective of this paper is to provide a review of various efforts that researchers have made to mathematically model the coupled heat and mass transfer process occurring within the wheel. The paper first briefly describes desiccant wheel including fundamental principle, heat and mass transfer mechanism and the method of model establishment. Then various models consisting of ideal assumptions, governing equations, auxiliary conditions, solution methods and main results are presented. The models can be classified into two main categories: (1) gas-side resistance (GSR) model; (2) gas and solid-side resistance (GSSR) model which can be further subdivided into pseudo-gas-side (PGS) model, gas and solid-side (GSS) model and parabolic concentration profile (PCP) model. It shows that GSSR models are higher in precision and more complex compared with GSR models. In addition, the simplified empirical models based on measured data are briefly discussed. This review is useful for understanding the evolution process and status quo of the mathematical model and highlighting the key aspects of model improvement such as taking account of pressure loss or air leakage.
© 2007 Elsevier Ltd. All rights reserved.

Keywords: Desiccant wheel; Mathematical model

*Corresponding author. Tel.: +86 21 3420 6548; fax: +86 21 3420 6548.
E-mail address: rzwang@sjtu.edu.cn (R.Z. Wang).

1364-0321/$ - see front matter © 2007 Elsevier Ltd. All rights reserved.
doi:10.1016/j.rser.2007.01.012

Contents

1. Introduction

Most of traditional vapor compression air conditioning system influences the environment in three aspects. First, the CFCs and HCFCs used as working fluids are ozone-depleting substances. Second, most of the refrigerants such as HCFCs are the global warming gases. Third, refrigeration system consumes energy which in general is produced from fossil fuel and related to release of pollutions. These polluting materials such as CO, SO_x, NO_x are harmful to the health of people. While desiccant wheel air conditioning systems offer a lot of significant advantages over other AC systems. A few remarkable advantages can be summarized as:

1. Water, a natural working fluid, is used as refrigerant. Desiccant materials such as silica-gel and zeolite are also environmental friendly.
2. Desiccant cooling system can be powered by low grade thermal energy sources such as solar energy, geothermic energy and waste heat. Hence the operating costs can be significantly reduced.
3. The system deals with the sensible and the latent loads, respectively, and can be utilized in various climates or environmental conditions.
4. It overcomes the discontinuous problem of the fixed bed desiccant cooling system.
5. Compared with the liquid desiccant system in which the liquid and air directly interact, the solid one is compact and less subject to corrosion.

Nomenclature

a	the distance in radial direction (m), Eq. (20)
A	channel cross section area (m^2)
A_V	transfer area per unit volume (m^2/m^3), Eq. (65)
B	outside atmospheric pressure (Pa), Eq. (26)
c_p	specific heat (J/kg K)
d_e	hydraulic diameter $d_e = 4A/P$, Eq. (83)
D_e	desiccant effective diffusivity (m^2/s), Eq. (123)
D_G	gas phase diffusivity (m^2/s), Eq. (116)
D_K	Knudsen diffusivity (m^2/s), Eq. (132)
D_O	ordinary diffusivity (m^2/s), Eq. (132)
D_S	surface diffusivity (m^2/s), Eqs. (108), (131)
f	desiccant fraction in the wall or in the matrix
f_{sp}/f_d	the mass of support materials/desiccant per length in a tube (kg/m), Eq. (32)
F_s	ratio of free flow area to cross section area of rotary wheel, Eq. (65)
h	air-side convective heat transfer coefficient ($W/m^2 K$)
h'	compound convective heat transfer coefficient ($W/m^2 K$), Eq. (83)
h_m	convective mass transfer coefficient (m/s), Eq. (47)
h_{fg}	heat of vaporization of water (J/kg)
H	enthalpy (J/kg)
k	thermal conductivity (W/m K)
K_y	gas-side mass transfer coefficient ($kg/m^2 s$)
K'_v	composite mass transfer coefficient ($kg/m^2 s$), Eq. (84)
L	actual process channel length (wheel thickness) (m)
Le	Lewis number
m	mass (kg)
$\dot{m}$	mass flow rate of the stream (kg/s)
$\dot{m}'$	rate of phase change per unit length (kg/m s), Eq. (42)
m'	mass flow rate of air per unit cross section area ($kg/m^2 s$), Eq. (65)
n	the number of the channel, Eq. (20)
NTU	number of transfer units, Eq. (91)
P	channel cross section perimeter (m)
q_{st}	heat of sorption (J/kg adsorbate)
r	radial displace or radius of the particle (m), Eq. (143)
r_1	radius of the matrix axis (m), Eq. (100)
r_2	radius of the rotary wheel (m), Eq. (100)
R	separation factor (reflecting desiccant isotherm shape), Eq. (16)
T	temperature (K)
t	time (s)
t_r	time required for a complete matrix rotation (s), Eq. (82)
u	air velocity (m/s)
V	the total volume of desiccant wheel (m^3), Eq. (107)
W	desiccant adsorption mass (kg adsorbate/kg adsorbent)
X_m	actual channel width (m), Eq. (20)
Y	humidity ratio (kg/kg)

Y_a	absolute humidity ratio of the air stream (kg water vapor/kg dry air)
Y_d	humidity ratio in equilibrium with the desiccant (kg water vapor/kg dry air)
Y_g	absolute humidity ratio of the air stream (kg water vapor/kg moist air)
Y_m	humidity ratio in equilibrium with the matrix (kg water vapor/kg dry air)
z	axial displace through matrix measured from period entrance (m)

Greek letters

Φ	relative humidity
η	fraction of phase change energy delivered directly to the air, Eq. (42)
ρ	density (kg/m^3)
σ	volume fraction, Eq. (53)
δ	the thickness of desiccant felt (m)
θ	time from the beginning of period (s), Eq. (82)
θ_j	duration of period j (s), Eq. (82)
ω	wheel rotate speed (r/h)
τ	tortuosity, Eq. (109)
ε_t	felt porosity, Eq. (131)
μ_j	dry matrix mass divided by dry fluid mass in the matrix in period j, Eq. (79)

Subscript

0	initial estate
1	the process air
2	the regeneration air
a	dry air
ad	air in desiccant pore, Eq. (116)
d	desiccant
eff	effective property, Eq. (140)
f	entire felt (matrix and pores), Eq. (139)
fd	dry solid felt material, Eq. (138)
fm	matrix part of felt, Eq. (138)
fp	pores (inter-particle voids), Eq. (138)
fs	dry solid felt material, Eq. (138)
g	gas including dry air and vapor
in	inlet condition, Eq. (5)
j	period index (during the period *j*), Eq. (77)
l	liquid water of frost, Eq. (52)
lc	local, Eq. (37)
m	matrix
s	surface, in gas phase adjacent to gel particles, Eq. (130)
sp	support materials, Eq. (30)
v	water vapor
vs	saturated water vapor, Eq. (26)
w	wall, Eq. (119)
ws	saturated water, Eq. (75)

Desiccant wheel found in the desiccant cooling system is widely acknowledged as the most critical part of the system, both in terms of cycle performance and system cost. It has been successfully used in many systems for dehumidification and enthalpy recovery. With the development of computer hardware and numerical methodology, mathematical models are being used to carry out critical investigations concerning on the desiccant wheel. The advantages of this method are that it takes less time and cost than experimental method for predicting the performance of a desiccant wheel. The second point is that the mathematical model can produce large volumes of results at virtually no added expense and it is very convenient to perform parametric research and optimization analysis. The third reason is that by experimental means, some parameters like that inside the tubes cannot be measured. The last but not the least reason is the fundamental physics and surface chemistry of rotary desiccant wheel, fixed desiccant equipment and enthalpy wheel are similar, so that other installations may be investigated too by utilizing the model of desiccant wheel [1–3]. Consequently, constructing valid mathematical model for desiccant wheel has become the key subject of many studies. Lots of mathematical models have been constructed and employed to analyze, develop and design desiccant wheels. However, to the authors' knowledge, there is not yet a work that summarizes comprehensively the numerous significant works done on modeling the desiccant wheel system. Hence, the objective of this article is to examine the progress in the area of mathematical modeling on the desiccant wheel.

Based on the heat and mass conservation principles, the combined heat and mass transfer in desiccant wheel can be formulated with complex mathematical detail as governing equations and auxiliary relations. This is the main and universal method for constructing mathematical model. There are also some simplified models for ease of computation such as pseudo-steady-state model [4,5], which are not fundamentally correct or universal. Moreover, it is an effective way to get the empirical performance fitted correlation using large amounts of experimental results. But its application is restricted in the specific range of experimental working conditions. The review of this paper will focus on the mainstream mathematical models. Besides, some empirical models will be briefly introduced too.

The first category of the paper is distinguished by whether the model gives solid-side resistance (SSR). Within the first section, it is ordered according to the dimension of models. For the second category, papers are grouped together by the method of calculating SSR. For each model reviewed, attempt has been made to gather up the assumptions, governing equations, auxiliary relations and the solution techniques for ensuring the integrality of the model. The results and validation of some models are listed when comparison between them are needed.

2. Problem description

2.1. *The fundamental principle*

Desiccant wheel is also known as dehumidification wheel, wheel dehumidifier or rotary dehumidifier in different literatures. The main components of desiccant wheel include matrix, clapboard, the wheel case, the air heater, the driven motor, etc. as shown in Fig. 1. Matrix usually contains supporting material and desiccant material. The case of desiccant wheel is driven by an engine and moves at a given rotary velocity. It consists of a large

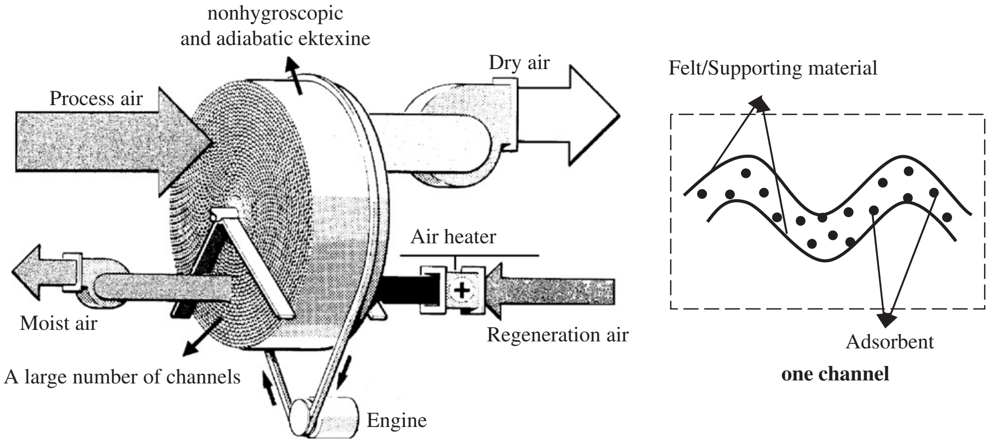


Fig. 1. Schematic figure of rotary desiccant wheel.

number of channels whose walls are constituted by supporting material and coated or impregnated with desiccant material. The cross section of wheel is divided into process air side and regeneration air side by the clapboard. Water vapor is adsorbed by the desiccant when moist air is passing through process air side. And while the hot air which is heated up by the heater flows through regeneration side, water is desorbed out from the desiccant and desiccant material is regenerated. The airflows can be either in counter-flow or co-current arrangement. It can be found that the reduction of moisture in the process air is at the price of the energy consumed to heat the regeneration air. This mode is called active desiccant wheel. If no air heater is built in system, the mode is named as passive desiccant wheel, enthalpy wheel or rotary energy wheel. It should be noted that the wheel is usually installed with thermal insulation and air proof material. Hence the energy and mass exchange between the wheel and environment is neglected in most cases.

2.2. *Mechanism of heat and mass transfer in desiccant wheel*

During adsorption, heat of sorption is released as desiccant adsorbs water vapor. The heat generated in the desiccant is transmitted through the material which decreases the sorption capacity. Therefore, the heat and mass transfer within the desiccant are coupled and should be considered simultaneously in developing mathematical model.

In a desiccant dehumidifier, there exist gas-side resistances (GSRs) and solid-side resistances (SSRs). GSRs come from diffusion and heat conduction within the air and convective heat and mass transfer between air and desiccant. It influences the heat and mass transfer from the air stream to the surface of the desiccant felt. Due to diffusion and heat conduction within the air is small in comparison with convective transfer, they are always neglected. SSRs come from heat conduction and mass diffusion within solid desiccant felt. Where the mass diffusion involves a number of physical mechanisms: (1) surface reaction combined with the adsorption process; (2) interparticle channel diffusion and adsorption within the layer; (3) micropore and macropore diffusion and adsorption within the desiccant particles [3].

2.3. Mathematical model establishment

The main steps to establish mathematical model include: (i) assumption proposal and selecting appropriate control volume; (ii) deriving the partial differential governing equations based on the mass and energy balances; (iii) providing auxiliary relation to close the governing equations; (iv) adopting proper mathematic approach to solve the model.

Some ideal assumptions are needed for the reason that:

(1) The mass and heat transfer occurring in the wheel are too complicated to understand completely.
(2) Some factors that do not influence heat and mass transfer significantly can be neglected. Then the complexity of the governing equations can be reduced and the solution is relatively simple and time-saving.

2.3.1. General governing equations

Euler cylindrical coordinate system has three coordinates: axial direction (z), radial direction (r) and circumferential direction (φ) and is usually employed to describe the wheel which has the same cylindrical geometry like Euler cylindrical coordinate system. In general, governing equations involve four main equations such as: mass and energy balance equations in the air and in the solid side. For clarity, the system is considered to be one-dimensional and explanations of main terms in governing equations are presented below. The physical model is shown in Fig. 2.

The moisture conservation in the air can be expressed as

$$d_e\rho_a\left(\frac{\partial Y_a}{\partial t}+u\frac{\partial Y_a}{\partial z}\right)=K_y(Y_d-Y_a). \tag{1}$$

The first term on the left-hand side (LHS) of the above equation is the moisture storage term in the air. The second term on the LHS represents the rate of moisture variation in the air due to the axial flow of the air. The first term on the right-hand side (RHS) of Eq. (1) expresses the rate of moisture variation in the air caused by the convective mass transfer.

The energy conservation for the air is described as

$$d_ec_{pa}\rho_a\left(\frac{\partial T_a}{\partial t}+u\frac{\partial T_a}{\partial z}-\frac{k_a}{c_{pa}\rho_a}\frac{\partial^2 T_a}{\partial z^2}\right)=h(T_d-T_a)+c_{pv}K_y(Y_d-Y_a)(T_d-T_a). \tag{2}$$

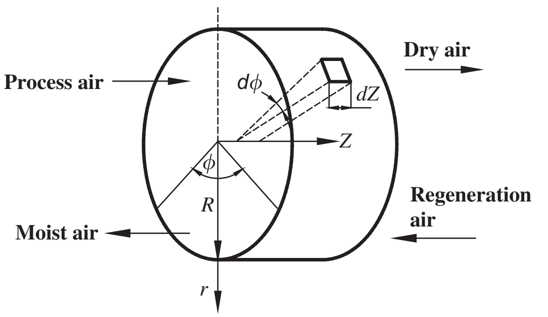


Fig. 2. Euler cylindrical coordinate system and a model of control volume of the desiccant wheel.

The first term on the LHS of the equation represents energy storage in the humid air. The second term on the LHS calculates the rate of energy variation in the air due to the axial flow of the air. The third term on the LHS represents the heat conduction in the air. The first term on RHS of Eq. (2) expresses the convective heat transfer between the air and solid desiccant. The second term on RHS of Eq. (2) indicates the sensible heat transfer between the air and solid desiccant.

The moisture conservation in desiccant is given by

$$\rho_d \delta \left(\frac{\partial W}{\partial t} - D_e \frac{\partial^2 W}{\partial z^2} \right) = K_y (Y_d - Y_a). \tag{3}$$

The first term on the LHS of the above equation is the moisture storage term inside desiccant. The second term on the LHS shows mass diffusion within the solid desiccant in axial direction. The first term on the RHS of Eq. (3) represents the convective mass transfer between the air and desiccant.

The energy conservation in desiccant can be written as follows:

$$c_{p_d} \rho_d \delta \left(\frac{\partial T_d}{\partial t} - \frac{k_d}{c_{p_d} \rho_d} \frac{\partial^2 T_d}{\partial z^2} \right) = h(T_a - T_d) + K_y (Y_a - Y_d) q_{st} + c_{pv} K_y (Y_a - Y_d)(T_a - T_d). \tag{4}$$

The first term on the LHS of the above equation is the energy storage term of desiccant. The second shows the heat transfer due to heat conduction within desiccant. The first term on the RHS of Eq. (4) calculates the convective heat transfer between the solid desiccant and air. The second term on the RHS expresses the influence of adsorption heat. The third term on the RHS expresses the sensible heat transfer between the solid desiccant and air.

It is important to note that in the above governing equations, it is assumed that all of the adsorption heat is delivered to desiccant.

2.3.2. *Auxiliary conditions and mathematical methods*

In order to close the partial difference equations, some auxiliary conditions have to be provided. They are boundary conditions, initial conditions for transient analysis, adsorption equilibrium correlations. Also, the values of adsorption heat q_{st}, convective transfer coefficient h, thermal conductivity k and moisture diffusivity D_e in desiccant material are need to give.

a. *Boundary conditions*: Boundary conditions describe the behavior of the simulation at the edges of the simulation region. The boundary conditions, commonly encountered in desiccant wheel model, are usually in three modes:

(I) Boundary conditions specify the values or the normal derivative of parameters on a surface [6], such as:
In the process/regeneration air ($i = 1$ for process air; $i = 2$ for regeneration air)

$$T_{a,\mathrm{in}} = T_{i,\mathrm{in}}, \tag{5}$$

$$Y_{a,\mathrm{in}} = Y_{i,\mathrm{in}}. \tag{6}$$

The insulated and impermeable boundaries result in [7]

$$\left.\frac{\partial T_m}{\partial r}\right|_{r=0} = \left.\frac{\partial T_m}{\partial z}\right|_{z=0} = \left.\frac{\partial T_m}{\partial z}\right|_{z=L} = 0, \tag{7}$$

$$\left.\frac{\partial Y_m}{\partial r}\right|_{r=0} = \left.\frac{\partial Y_m}{\partial z}\right|_{z=0} = \left.\frac{\partial Y_m}{\partial z}\right|_{z=L} = 0. \tag{8}$$

(II) Periodic boundary conditions: The periodic boundary conditions at $\Phi = 0$ [8]

$$\begin{cases} Y_a(0,z,t) = Y_a(2\pi,z,t), \\ T_a(0,z,t) = T_a(2\pi,z,t), \\ W(0,z,t) = W(2\pi,z,t), \\ T_d(0,z,t) = T_d(2\pi,z,t). \end{cases} \tag{9}$$

The periodic equilibrium boundary conditions expressed in the form of limitation [9]:
for $0 \leqslant z \leqslant L$

$$\begin{cases} \lim\limits_{\theta_1 \to \theta_j^-}\left[W_m\left(\frac{z}{L}, t_1\right)\right] = \lim\limits_{\theta_2 \to 0^+}\left[W_m\left(1-\frac{z}{L}, t_2\right)\right], \\ \lim\limits_{\theta_1 \to \theta_j^-}\left[H_m\left(\frac{z}{L}, t_1\right)\right] = \lim\limits_{\theta_2 \to 0^+}\left[H_m\left(1-\frac{z}{L}, t_2\right)\right], \\ \lim\limits_{\theta_1 \to 0^+}\left[W_m\left(\frac{z}{L}, t_1\right)\right] = \lim\limits_{\theta_2 \to \theta_j^-}\left[W_m\left(1-\frac{z}{L}, t_2\right)\right], \\ \lim\limits_{\theta_1 \to 0^+}\left[H_m\left(\frac{z}{L}, t_1\right)\right] = \lim\limits_{\theta_2 \to \theta_j^-}\left[H_m\left(1-\frac{z}{L}, t_2\right)\right]. \end{cases} \tag{10}$$

(III) Boundary conditions depict heat and mass transfer on a surface [10]

$$\rho_{fp} D_G \frac{\partial Y_d}{\partial r}(t,z,0) + \rho_d D_S \frac{\partial W}{\partial r}(t,z,0) = 0, \tag{11}$$

$$-\rho_{fp} D_G \frac{\partial Y_d}{\partial r}(t,z,a_d) - \rho_d D_S \frac{\partial W}{\partial r}(t,z,a_d) = K_y[Y_d(t,z,a_d) - Y_a(t,z)], \tag{12}$$

$$k_d \frac{\partial T_d}{\partial r}(t,z,0) = \rho_w \delta c_{pw} \frac{\partial T_w}{\partial t}, \tag{13}$$

$$-k_d \frac{\partial T_d}{\partial r}(t,z,a_d) = h[T_d(t,z,a_d) - T_a(t,z)]. \tag{14}$$

b. *Initial conditions*: Initial conditions give the value of parameters at a given starting time ($t = 0$). For example, the initial condition of parameter X is

$$X(t=0) = X_0. \tag{15}$$

X is replaced by the detailed parameters in different models.

c. *Equilibrium adsorption equation*: The equilibrium equation determines the amount of moisture that will be adsorbed by the desiccant. Emphasis should be placed on the fact that adsorption is a dynamic process. With different operation conditions, such as relative humidity of the air in equilibrium with the adsorbent Φ, desiccant temperature T_d, etc., desiccant has different adsorption capacity and equilibrium adsorption quantity. Up to now, through experiments to obtain the dynamic adsorption data and equilibrium equation for different desiccants is the main method. As a result, there are many types of equilibrium adsorption relationships including: relative humidity of moist air in equilibrium with the adsorbent Φ and separation factor R are used to calculate the water content of the adsorbent W:

$$W/W_{\max} = \Phi/[R + (1 - R)\Phi]. \tag{16}$$

Some researchers consider that W is the function of Φ and temperature of moist air in equilibrium with the adsorbent T_d:

$$W = f(T_d, Y_d) = f'(T_d, \Phi). \tag{17}$$

Sometimes it is assumed that the W is a function of Φ only and invariable with temperature T_d:

$$W = f(\Phi). \tag{18}$$

Besides, the following relationship is utilized in many works:

$$\Phi = f(W, W_{\max}, R, h^*, P_{ws}). \tag{19}$$

d. *Mathematical solution*: Due to the complexity and nonlinearity of such coupled heat and mass transfer models, it is difficult to obtain analytical solutions. Hence numerical methods have been applied to solve the partial differential governing equations. At present, the most widely used solution method for desiccant wheel model is finite difference method. Other methods such as finite volume method [7] and analogy method [11,12] have also been used in some works.

3. Gas-side resistance (GSR) model

In early research, due to the lack of study on complex diffusion mechanism inside solid desiccant, the heat and mass transfer processes from air stream to desiccant are thought to be controlled by GSRs only. Gradients of temperature and concentration within solid desiccant are ignored. Thus the second terms on the LHS of Eqs. (3) and (4) are omitted. Some researchers only consider the transfer processes in axial direction. Others consider that in axial as well as circumferential direction.

3.1. One-dimensional model

To save the computation time, it is desired to take into account as less dimension as possible in the model. Since the variation in moisture as well as temperature is more significant in axial direction, it is often chosen as main direction for heat and mass transfer in constructing the governing equations. Usually, condensation is not considered in the models. However, it happens in certain conditions. Hence some researchers include it in their models.

3.1.1. Models without considering condensation

Charoensupaya and Worek [13] have derived a simple one-dimensional dehumidifier model based on the following ideal assumptions:

1. The axial direction (z) heat conduction and molecular diffusion within the desiccant coating were negligible.
2. There were no radial direction (r) temperature or moisture content gradients in the matrix.
3. The axial direction heat conduction and water vapor molecular diffusion in the air were negligible.
4. The inlet air conditions were uniform radially, but might vary with time.
5. The tubes that make up the rotary desiccant wheel were identical.
6. All the channels were assumed to be adiabatic and impermeable.
7. The effect of centrifugal force was neglected.
8. The thermophysical properties of the dry air and the properties of the dry desiccant material as well as the matrix were constant.
9. The pressure and velocity losses of the air stream in the axial direction were negligible.
10. The heat and mass transfer coefficients between the air stream and the desiccant wall were constant over the entire dehumidifier.

It can be inferred from the assumptions 1 and 2 that this model neglects the SSRs. Because of symmetry characteristic, the middle of one tube could be considered adiabatic and half size of the channel was selected as the differential control volume as can be seen in Fig. 3.

The channel was assumed to be adiabatic and impermeable, hence the conservation of moisture and energy between the process air stream and matrix were

$$\rho_a a_a \frac{\partial Y_a}{\partial t} + \frac{\dot{m}_a}{nX_m}\frac{\partial Y_a}{\partial z} + f\rho_m 2\delta \frac{\partial W}{\partial t} = 0, \tag{20}$$

$$\frac{\dot{m}_g}{X_m}\left(\frac{1}{u}\frac{\partial H_g}{\partial t} + \frac{\partial H_g}{\partial z}\right) + \frac{m_m}{X_m L}\frac{\partial H_m}{\partial t} = 0. \tag{21}$$

Conservation of moisture in the matrix was

$$\frac{fm_m}{nX_m L}\frac{\partial W}{\partial t} = 2K_y(Y_a - Y_m), \tag{22}$$

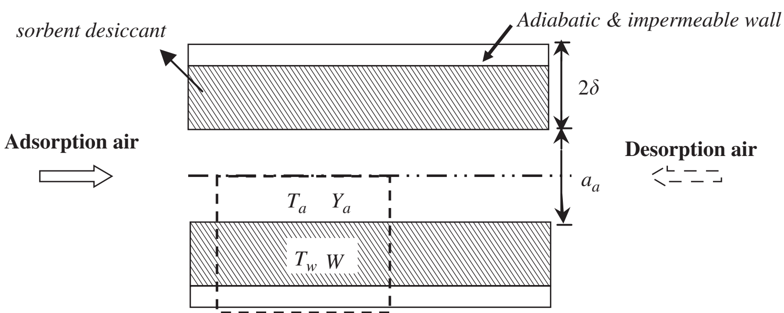


Fig. 3. A model of dehumidifier differential element for GSR model [13].

where m_m is the total mass of the matrix in the dehumidifier

$$m_m = 2\delta \rho_m n X_w L. \tag{23}$$

Conservation of energy in the air was calculated by:

$$\frac{\dot{m}_g}{nX_m}\left(\frac{1}{u}\frac{\partial H_g}{\partial t} + \frac{\partial H_g}{\partial z}\right) = 2K_y(Y_m - Y_a)\frac{\partial H_g}{\partial Y_a} + 2h(T_m - T_a), \tag{24}$$

where $\partial H_m/\partial W$ means the differential heat of wetting and $\partial H_g/\partial Y_a$ is defined as

$$\frac{\partial H_g}{\partial Y_a} = q_{st} + \frac{1}{f}\frac{\partial H_m}{\partial W}. \tag{25}$$

The subscript "*m*" in the above equations means the matrix including nonhygroscopic exterior surface, support materials and the desiccant. Parameters n, X_m and L represent holistic configuration of the wheel. The governing equations were solved subject to the equilibrium relation, Eq. (16). It was supposed that the variation of adsorption heat q_{st} did not influence system performance greatly, hence q_{st} was taken as constant and the average value of 2700 kJ/kg H_2O was used.

Then the models were converted into nondimensional form and solved numerically using an explicit finite-difference method. This model had been used to calculate an open-cycle, adiabatic, solid desiccant cooling system operating in the ventilation mode. The system used an adiabatic dehumidifier, a regenerative heat exchanger whose effectiveness was 0.95, and two direct evaporative coolers with effectiveness of 0.95. The effects of dehumidifier channel length, desiccant mass fraction and desiccant isotherm shape on system performance in terms of COP were investigated. The results showed that there are optimum mass fraction and desiccant isotherm shape which will result in an optimum COP. Furthermore, the desiccant cooling system operating in the ventilation mode can yield COP as high as 1.4.

Zheng and Worek [14] have established a transient one-dimensional desiccant wheel model which has similar assumptions and control volume as those of Charoensupaya and Worek [13], with certain modifications. They omitted the storage terms $\partial Y_a/\partial t$ and $\partial H_g/\partial t$ in Eqs. (20), (21), (24) and adopted the enthalpy of water vapor to replace $\partial H_g/\partial Y_a$ in Eq. (24).

The new governing equations were subject to boundary condition of Eqs. (5), (6) and initial conditions with parameter Y_w and T_w. The relationship between humidity ratio and relative humidity was described as

$$Y_d = \frac{0.62198 P_v}{B - P_v} = \frac{0.62198 \Phi_d}{B/P_{vs} - \Phi_d}, \tag{26}$$

where P_{ws} presents the saturation pressure of water vapor

$$P_{ws} = \exp\left(\frac{\lambda_1}{T} + \lambda_2 + \lambda_3 T + \lambda_4 T^2 + \lambda_5 T^3 + \frac{\lambda_6}{\ln T}\right),$$

$$\begin{cases} \lambda_1 = -5800.2206; \lambda_2 = 1.3914933; \lambda_3 = -0.04860239, \\ \lambda_4 = 0.41764768 \times 10^{-4}; \lambda_5 = -0.14452093 \times 10^{-7}; \lambda_6 = 6.5459673. \end{cases} \tag{27}$$

The following empirical form was used to give heat of sorption [15]:

$$\frac{q_{st}}{h_{fg}} = h^*(W/W_{\max}) = 1 + \Delta h^* \frac{\exp(\lambda W/W_{\max}) - \exp(\lambda)}{1 - \exp(\lambda)} \quad \lambda = \text{constant}, \tag{28}$$

where h_{fg} is the heat of vaporization of water.

The equilibrium equation was represented by

$$\Phi = \frac{WR}{W_{\max} + (R-1)W} \left[\frac{P_{vs}(T)}{P_{vs}(T_0)}\right]^{h^*-1}. \tag{29}$$

And the enthalpy of desiccant bed was expressed by

$$H_m = (1-f)c_{psp}T_m + f\left[c_{pd}T_m + \int_0^W (H_v - q_{st})\,\mathrm{d}W\right]. \tag{30}$$

The simulation aimed to study different numerical methods. They adopted an implicit scheme finite difference method with variable step sizes in time and space coordinates to solve the governing equations. It has been reported that compared with explicit scheme, the implicit scheme is unconditionally stable, is of high-order accuracy, and enables more rapid calculation of dehumidifier performance with much larger time and space steps. Meanwhile, the simulation program was validated by two methods: (i) varying step sizes in both space and time; (ii) comparing with other available works, such as results of Ref. [13]. Both validation methods verified the convergence and accuracy of the model. Using this model, the effect of rotation speed on the performance of the adiabatic desiccant wheel was parametrically studied, and the optimal rotational speed was discovered by examining outlet humidity profiles of the adsorption-side as well as humidity wave fronts inside the desiccant dehumidifier.

Moreover the same model was used: (i) to optimize the wheel rotational speed [16]; (ii) to investigate the influences of desiccant sorption properties, heat and mass transfer characteristic and the size of the wheel on the dehumidification performance of the desiccant wheel [17]; (iii) and to investigate the wheel performance at the real operating conditions which vary significantly from the design point (i.e., at ARI conditions) [18].

Zhang et al. [6,19,20] constructed a mathematical model of a honeycombed desiccant wheel. The tube with honeycombed geometry and differential control volume are shown in Figs. 4 and 5. Heat of sorption was considered to be delivered to the matrix only. And the channel was assumed to be impermeable but not adiabatic. Hence, the model consisted of conservation equations of moisture and heat in the air (Eqs. (31) and (33)) and within desiccant (Eqs. (32) and (34)) separately, which are different form the governing equations (20) and (21).

$$A\rho_a\left(\frac{\partial Y_a}{\partial t} + u\frac{\partial Y_a}{\partial z}\right) = K_y P(Y_d - Y_a), \tag{31}$$

$$\frac{1}{2} f_d \frac{\partial W}{\partial t} = K_y P(Y_a - Y_d), \tag{32}$$

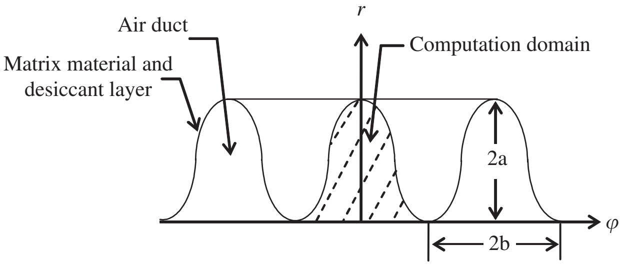


Fig. 4. Corrugated air duct and the computation domain of a GSR model [19].

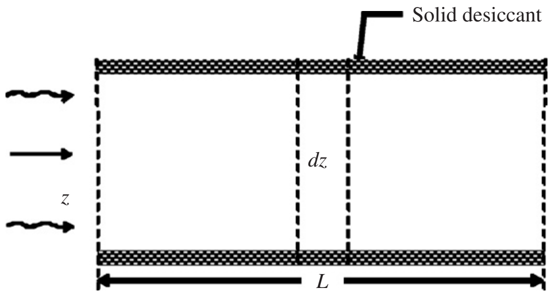


Fig. 5. The differential control volume in the corrugated duct [19].

$$A\rho_a(c_{pa}+Y_ac_{pv})\left(\frac{\partial T_a}{\partial t}+u\frac{\partial T_a}{\partial z}\right)=hP(T_d-T_a)+K_yPc_{pv}(Y_{\mathrm{d}}-Y_{\mathrm{a}})(T_d-T_a), \tag{33}$$

$$\frac{1}{2}[f_d(c_{pd}+Wc_{pl})+f_{sp}c_{psp}]\frac{\partial T_d}{\partial t} = hP(T_a-T_d)+K_yP(Y_a-Y_d)q_{st}+K_yPc_{pv}(Y_a-Y_d)(T_a-T_d). \tag{34}$$

The adsorption heat of RD silica gel was calculated by the following equation [15]:

$$q_{st}=h_{fg}[1.0+0.2843\exp(-10.28W)]. \tag{35}$$

The equilibrium relative humidity on the surface of RD silica gel was obtained by fitting fourth-degree polynomials to the test data provided by manufacturer [21]

$$\Phi=0.0078-0.05759W+24.16554W^2-124.478W^3+204.226W^4. \tag{36}$$

The relationship between humidity ratio and relative humidity was described as Eq. (26). The pressure of saturated water vapor P_{vs} was given by Antonine equation:

$$P_{vs}=\exp\left(23.196-\frac{3816.44}{T_d-46.13}\right). \tag{37}$$

In addition, convective heat and mass transfer coefficients were determined by [22]

$$h = \frac{Nu_{lc} k_a P}{4A}, \tag{38}$$

$$K_y = \rho_a \frac{Sh_{lc} D_a P}{4A}, \tag{39}$$

where

$$Nu_{lc} = Sh_{lc}, \tag{40}$$

$$D_a = 2.302 \times 10^{-5} \frac{P_0}{P_a} \left(\frac{T_a}{T_0}\right)^{1.81}, \quad P_0 = 0.98 \times 10^{-5} P_a, \quad T_0 = 256\,\mathrm{K}, \tag{41}$$

where D_a is the mass diffusion diffusivity of water vapor in the air.

The model was solved by backward implicit difference scheme and validated by experimental results of a real honeycombed paper-based silica gel desiccant wheel. A good agreement was obtained between the calculation results and the experimental data. Using the model, the temperature and humidity ratio profiles in the wheel during both the dehumidification and regeneration processes were analyzed [20]. The results indicated that a hump curve of air humidity ratio along the channel existed all the time in the regeneration side. The performance of desiccant wheel was significantly affected by the hump curve. In order to improve the performance of the desiccant wheel, it was essential to accelerate the hump moving from the duct entrance to the duct exit as quickly as possible. Also the effects of velocity and inlet temperature of regeneration air and velocity of process air on the hump moving speed were investigated too. It was found that increasing the velocity and inlet temperature of regeneration air could accelerate the hump moving. Meanwhile the velocity of process air had little influence on the hump.

Simonson and Besant [7] have presented a numerical model for coupled heat and moisture transfer during adsorption and desorption processes. Although proposed for rotary energy wheel, the model is still listed here because: (1) desiccant wheel and rotary wheel have similar operation and function of transferring heat and moisture; (2) a new factor η is proposed in their model to account for the distribution of phase change energy between the desiccant and the air. The tube geometry cross-section and limited simplifying assumptions are basically similar to those of Zhang [6].

One tube is chosen as the control volume (Fig. 6). The conservation of energy in the air is given by

$$\rho_g c_{pg} A \frac{\partial T_g}{\partial t} + u \rho_g c_{pg} A \frac{\partial T_g}{\partial z} = \dot{m}' q_{st} \eta + hP(T_m - T_g), \tag{42}$$

where η is the fraction of the phase change energy entering the air. And then the first term on the RHS of above equation calculates the heat of sorption delivered to the air side.

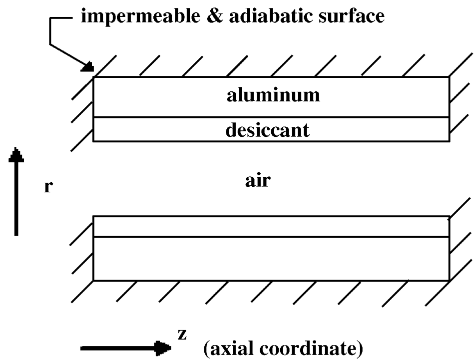


Fig. 6. Side view of rotary energy exchanger duct showing the aluminum surface [7].

The conservation of energy in the matrix (subscript "m", including aluminum, desiccant and moisture) is described by

$$\rho_m c_{pm} A_m \frac{\partial T_m}{\partial t} - \frac{\partial}{\partial z}\left(k_{\mathrm{al}} A_{\mathrm{al}} \frac{\partial T_m}{\partial z}\right) = \dot{m}' q_{st}(1-\eta) + \dot{m}' c_{pl}(T_g - T_m) + hP(T_g - T_m). \tag{43}$$

It is supposed that the heat conduction through the matrix in the axial direction is dominated by the conduction through aluminum surface layer (subscript "al") which is expressed by the second term on the LHS of Eq. (43). The first term on the RHS calculates the rest heat of sorption delivered to the matrix. The second on the RHS shows the sensible heat transfer between the solid desiccant and air.

Conservation of mass in the air results in two equations, one for the dry air and another for water vapor, which is different from the general governing equation (1):

$$A \frac{\partial \rho_v}{\partial t} + \frac{\partial}{\partial z}(\rho_v u A) = -\dot{m}', \tag{44}$$

$$\frac{\partial \rho_a}{\partial t} + \frac{\partial}{\partial z}(\rho_a u) = 0. \tag{45}$$

Conservation of mass in the matrix is given as

$$\rho_{d,\mathrm{dry}} A_d \frac{\partial W}{\partial t} = \dot{m}', \tag{46}$$

where "$\dot{m}'$" means the rate of phase change per unit length

$$\dot{m}' = h_m P(\rho_v - \rho_{v,m}), \tag{47}$$

where ρ_v and $\rho_{v,m}$ stand for water vapor density and water vapor density on the desiccant surface. The following equation is used to calculate the value of $\rho_{v,m}$:

$$\rho_{v,m} = \frac{P_{ws}(T_m)}{R_v T_m} \frac{W}{(W_m - W)C}, \quad 0 \leqslant W \leqslant W_m \frac{C}{1+C}, \tag{48}$$

where P_{vs} is saturation vapor pressure and calculated by

$$P_{vs} = \exp(F),$$
$$F = \begin{cases} \dfrac{C_1}{T} + C_2 + C_3T + C_4T^2 + C_5T^3 + C_6T^4 + C_7 \ln T, & 173\,\mathrm{K} < T < 273\,\mathrm{K}, \\ \dfrac{C_8}{T} + C_9 + C_{10}T + C_{11}T^2 + C_{12}T^3 + C_{13} \ln T, & 273\,\mathrm{K} < T < 473\,\mathrm{K}. \end{cases} \tag{49}$$

Heat of sorption is given by

$$\frac{q_{st}}{h_{fg}} = h^*(W/W_{\max}) = 1 + \Delta h^*\left(1 - \frac{W}{W_{\max}}\right)^{\lambda}, \quad \lambda = f(W), \tag{50}$$

where λ describes the shape of heat of sorption as a function of moisture content.

The geometry and property relations for the moist air (g), desiccant (d) and matrix (m) are

$$c_{pg}\rho_g = \rho_a c_{pa} + \rho_v c_{pv}, \tag{51}$$

$$\rho_d = \rho_{d,\mathrm{dry}}(W + 1), \quad c_{pd}\rho_d = \rho_{d,\mathrm{dry}}(Wc_{pl} + c_{p,\mathrm{dry}}), \tag{52}$$

$$\rho_m = \sigma_d\rho_d + \sigma_{\mathrm{al}}\rho_{\mathrm{al}}, \quad c_{pm}\rho_m = \rho_m = \sigma_d\rho_d c_{pd} + \sigma_{\mathrm{al}}\rho_{\mathrm{al}}c_{pal}, \tag{53}$$

$$\sigma_d + \sigma_{\mathrm{al}} = 1. \tag{54}$$

The convective heat transfer coefficient h in Eqs. (42), (43) was obtained from numerical simulations of simultaneously (thermal and hydrodynamic) developing flow in an equilateral triangular duct [23]. Convective mass transfer coefficient h_m in Eq. (47) was determined by using the analogy between heat and mass transfer. The boundary conditions for the problem included Eqs. (5) and (7) and

$$\rho_{a,\mathrm{in}} = \rho_{i,\mathrm{in}}, \quad \rho_{v,\mathrm{in}} = \rho_{i,v,\mathrm{in}}, \quad u_{\mathrm{in}} = u_{i,\mathrm{in}}. \tag{55}$$

The governing equations were discretized by finite volume method with a staggered grid [24]. Upwind difference scheme and central differencing were used in the air and matrix, respectively. Transient terms and source terms were treated in fully implicit and semi-implicit manner. The discretized equations were solved using a Gauss–Seidel iteration technique with under relaxation.

The model was validated by comparing its results with the experimental data of a commercial molecular sieve rotary energy exchanger by Simonson and Besant [25]. It has been reported that the measured and simulated results agreed well within experimental uncertainty. Besides, the effects of some important factors, such as phase change term η, adsorption heat and isotherm, axial heat conduction in matrix, storage in air and entry length, on the predicted performance of molecular sieve energy wheel were discussed. The predicted effectiveness was found to be greatly influenced by the value of η.

3.1.2. Models considering condensation

In the above models, the desiccant wheels are formulated at or near atmospheric pressure, where no condensation happens. When desiccant wheel works under high

pressure, condensation might occur in the regeneration process. The models reviewed in this part are capable of properly simulating desiccant wheel operating at high pressures.

In order to analyze the performance of an adiabatic desiccant wheel under high process and regeneration air stream pressures, Mihajlo and William [26] have derived a model containing two groups of governing equations, one for the noncondensation situation and another for the case when condensation occurred. The ideal assumptions, governing equations for noncondensation situation and auxiliary relations are similar to that of Zheng and Worek [14]. A new set of governing equations were constructed when condensation happened such as:

Conservation of moisture in the process air:

$$\rho_a a_p u \frac{\partial Y_a}{\partial z} = 2K_y(Y_m - Y_a) - \frac{2h(T_a - T_m)}{h_{fg}}. \tag{56}$$

Conservation of moisture in the matrix:

$$f\rho_m \delta \frac{\partial W}{\partial t} = 2K_y(Y_a - Y_m) + \frac{2h(T_a - T_m)}{h_{fg}}. \tag{57}$$

The temperature of air which was saturated with water vapor was taken as constant

$$T_a = \text{constant}. \tag{58}$$

Conservation of energy in the matrix

$$\rho_m \delta \frac{\partial H_m}{\partial t} = 2q_{st}K_y(Y_a - Y_m) + q_{st}\frac{2h(T_a - T_m)}{h_{fg}}. \tag{59}$$

An implicit finite-difference scheme was adopted to solve the model. The performance analysis using this model revealed that: (1) the value of optimal separation factor R under high pressure is greater than that under atmospheric pressure; (2) if the regeneration temperature T_{reg} is between 65 and 100 °C and R is between 0.01 and 0.1, condensation could occupy 21–40% of regeneration section of the wheel; (3) only for R larger than 0.4 does condensation not happen.

A similar extension of the model [6] was conducted by Zhong [27], to include condensation process. Similarly, two sets of governing equations were established, respectively, for the condensation process and noncondensation process. The assumptions, governing equations of noncondensation status, auxiliary relations and solution method were similar to that of Zhang [6]. The derived model of condensation process consisted of:

Conservation of moisture in the process air:

$$A\rho_a\left(\frac{\partial Y_a}{\partial t} + u\frac{\partial Y_a}{\partial z}\right) = K_yP(Y_d - Y_a) + \frac{hP(T_d - T_a)}{h_{fg}}. \tag{60}$$

Conservation of moisture in the desiccant:

$$\frac{1}{2}f_d\frac{\partial W}{\partial t} = K_yP(Y_a - Y_d) + \frac{hP(T_a - T_d)}{h_{fg}}. \tag{61}$$

Conservation of energy in the process air:

$$A\rho_a(c_{pa} + Y_a c_{pv})\left(\frac{\partial T_a}{\partial t} + u\frac{\partial T_a}{\partial z}\right) = hP(T_d - T_a) + K_y P c_{pv}(Y_d - Y_a)(T_d - T_a). \quad (62)$$

Conservation of energy in the desiccant:

$$\begin{aligned}\frac{1}{2}[f_d(c_{pd} + Wc_{pl}) + f_{sp}c_{psp}]\frac{\partial T_d}{\partial t} \\ = hP(T_a - T_d) + K_y P(Y_a - Y_d)q_{st} \\ + K_y P c_{pv}(Y_a - Y_d)(T_a - T_d) + \frac{hP(T_a - T_d)}{h_{fg}}q_{st}.\end{aligned} \quad (63)$$

This model was carried out to discuss the performance of RD silica gel desiccant wheel under high pressure. It has been reported that when the separation factor R is 0.01, operating pressure almost had no effect on desorption capacity, but sorption capacity enhanced with increasing pressure. Especially if the pressure is higher than 3 atm, the sorption capacity could be greatly improved. When R reaches 1, the adsorption capacity is enhanced and desorption capacity gets worse with pressure rising. If the pressure is higher than 3 atm, the variation of adsorption capacity is not significant. It was also found that desiccant wheel achieves a better performance at the condition of $R = 1$ as compared to $R = 0.01$.

Condensation and frosting processes occurring in energy wheels have been investigated too. Simonson and Besant [28] expanded the model proposed by them [7] to include condensation and frosting processes. The difference between the governing equations of these two models is that the adsorption heat q_{st} in Eqs. (42) and (43) is replaced by heat of vaporization h_{fg}. In saturation condition, the density of water vapor can be approximated by

$$\rho_v = \rho_{vs} = \frac{P_{vs}}{R_v T_g}, \quad (64)$$

where R_v is the specific gas constant of water vapor.

The numerical schemes are similar to those used in Ref. [7]. Mathematically and physically the problem becomes more complex when condensation and frosting are included. Hence these conditions require a different numerical solution strategy and then different algorithms are adopted during sorption and saturation process as shown in Table 1. This model could simulate the condensation and frosting happening in energy wheel. The solutions were validated by comparing the simulated results with experimental data on a commercial energy wheel. This study analyzed the sensitivity of condensation and frosting to wheel speed and desiccant type. The simulation results showed that a desiccant with a linear sorption curve has smaller amounts of condensation/frosting compared with Type I sorption curve.

Dimensionless equations of air-to-air energy wheel were derived using this model [29]. It was indicated that the performance of energy wheel is a function of the operating temperature and humidity. In addition, based on this model, Jeong and Stanley [30]

Table 1
Different algorithms used to solve the governing equations [28]

Sorption ($\Phi < 100\%$)	Common	Saturation ($\Phi = 100\%$)
	1. Estimate the rate of phase change and the properties needed in the governing equations	
2. Solve the T_m, ρ_v, W, u and T_g fields in order with Eqs. (42)–(46)		2. Solve the T_m, $\dot{m}'$, W, u and T_g fields in order with Eqs. (42)–(46)
	3. Update the properties	
4. Update the rate of phase change ($\dot{m}'$)		4. Update the rate of phase change (ρ_v)
	5. Return to step 2 and iterate until a converged solution is reached 6. Adjust, as necessary, the algorithm used in each grid for the next time-step 7. Increment time, return to step 2 and iterate until a quasi-steady solution is obtained	

Table 2
Features of gas side resistance (GSR) model reviewed in present work

Ref	Dimension	Condensation	Boundary conditions		Parameters of initial condisions	Other relations
			Mode	*Expressions*		
[13]	I		–	–	–	Eqs. (16), (25)
[14]	I		I	Eqs. (5), (6)	T_w Y_w	Eqs. (26)–(30)
[6]	I		I	Eqs. (5), (6)	T_a Y_a T_d Y_d W	Eqs. (26), (35)–(41)
[7]			I	Eqs. (5), (7), (55)	–	Eqs. (47)–(54)
[26]	I	√	I	Eqs. (5), (6)	T_w Y_w	Eqs. (26)–(30)
[27]	I	√	I	Eqs. (5), (6)	T_a Y_a T_d Y_d W	Eqs. (26), (35)–(41)
[28]	I	√	–	Eqs. (5), (7), (55)	–	Eqs. (47)–(54), (64)
[8]	II		I	Eqs. (5), (6)	T_a Y_a T_d W	–
			II	Eq. (9)		

developed practical enthalpy wheel effectiveness correlations which can be more easily used to design and analyze passive wheel.

3.2. Two-dimensional model

Multi-dimensional mathematical models reflecting the effects in radial or circumferential directions could be used to analyze heat and mass transfer processes comprehensively with improved accuracy. But the complexity increases simultaneously. Usually two-dimensional model is recognized as a compromise method between accuracy and complexity.

Yu et al. [8] have derived a two-dimensional GSR model. Convection items $\partial Y/\partial \varphi$, $\partial W/\partial \varphi$ and $\partial T/\partial \varphi$ in circumferential direction which reflect the heat and mass transfer

due to the rotation of the wheel were added into the model. The control volume of the model was the same as that shown in Fig. 2. The governing equations were as follows:

Conservation of moisture in the air:

$$\frac{\partial Y_a}{\partial t} + \omega \frac{\partial Y_a}{\partial \varphi} + \frac{m_i'}{\rho_i F_s} \frac{\partial Y_a}{\partial z} = \frac{K_y A_V}{\rho_i F_s}(Y_d - Y_a). \quad (65)$$

Conservation of moisture in the desiccant:

$$\frac{\partial W}{\partial t} + \omega \frac{\partial W}{\partial \varphi} = \frac{K_y}{\rho_d \delta}(Y_a - Y_d). \quad (66)$$

Conservation of energy in the air equation:

$$\frac{\partial T_a}{\partial t} + \omega \frac{\partial T_a}{\partial \varphi} + \frac{m_i'}{\rho_i F_s} \frac{\partial T_a}{\partial z} = \frac{h A_V}{\rho_i F_s (c_{pa} + Y_a c_{pv})}(T_d - T_a). \quad (67)$$

Conservation of energy in the desiccant:

$$\frac{\partial T_d}{\partial t} + \omega \frac{\partial T_d}{\partial \varphi} = \frac{h}{\rho_d \delta (c_{pd} + W c_{pl})}(T_a - T_d) + \frac{K_y (Y_a - Y_d) q_{st}}{\rho_d \delta (c_{pd} + W c_{pl})}. \quad (68)$$

Boundary conditions of modes I and II were introduced to solve the problem. The governing equations were discretized into finite difference equation group. For space varying items, one order upwind difference scheme was adopted for convection terms. For time variation items, different schemes were used according to the demands of computation. To compute steady state, fully implicit scheme was employed because of its reliability of convergence. To investigate the dynamic behavior of the dehumidification device, explicit scheme which does not need the iteration process was recommended. Owing to the constraints of stability, time step should be small enough, or the divergence of solution cannot be avoided. Moreover, small time step was also numerically necessary for accurate computation. Crank–Nicolson scheme could be carried out for dynamic investigation too. A proper mesh size should be specified to save computation time. It was found that the predicted result of this model is more close to the actual process than that of Charoensupaya and Worek [13]. This is mainly because although the convection items in circumferential direction can be neglected under low rotation speed, they influence heat and mass transfer process in almost all occasions. Hence, when they are added to the model, more practical results can be achieved compared with one-dimensional model. Also the analytic results indicated that when the density of the adsorbent ρ_d is smaller than 0.2, the influences of $\partial Y/\partial \varphi$ and $\partial T/\partial \varphi$ cannot be negligible.

Feng et al. [31] applied analogy method to solve the proposed governing equations by Yu et al. [8]. Their study have shown that the performance of dehumidifier is a function of the nondimensional structure parameters and thermophysical property parameters (such as nondimensional rotation period $t_r' = (m_a \bullet t_r)/(\rho_a \bullet F_s \bullet L)$, nondimensional moisture ratio $m' = (\rho_a \bullet F_s \bullet Y_a)/(W_{\max} \bullet M_w)$) with the operation parameters keeping constant. The GSR models summarized in this part are reviewed in Table 2.

4. Gas and solid-side resistance (GSSR) model

The previously mentioned GSR models do not consider the heat conduction and mass diffusion within solid side, thus they do not reflect the actual transfer process occurring in

Table 3
Features of gas and solid side resistance (GSSR) models reviewed in present work

Refs.	Dimension	Conduction in solid-side			Diffusion in solid-side			Boundary conditions		Parameters of initial conditions	Other relations
		z	r	φ	z	r	φ	Mode	Expressions		
[32]	I	PGS model						I	Eqs. (5), (6)	–	Eqs. (26), (75), (76)
								II	Eq. (9)		
[9]	I	PGS model						–	–	–	Eqs. (28), (83)–(88)
[33]	I	PGS model (ε-NTU Model)						II	Eq. (10)	Y_a H_g	Eqs. (93)–(95)
[34]	I	PGS model (Radial-flow wheel)						I	Eqs. (5), (6)	T_a Y_a	Eqs. (35), (96), (98), (105), (106)
								II	Eqs. (103), (104)		
[35]	I	√			√			–	–	–	Eqs. (35), (96), (109), (112)–(114)
[10]	II		√			√		III	Eqs. (11)–(14)	T_d Y_d	Eqs. (119)–(121)
[36]	II	√		√	√		√	I	Eqs. (5), (6)	T_a Y_a T_d W	Eqs. (26), (36), (126)–(128)
								II	Eq. (9)		
[37]	II	√	√		√	√		I	Eqs. (5)–(8)	—	Eqs. (129), (132), (135)–(137)
								III	Eqs. (12), (14)		
[38]	I/II/III	√	√	√	√	√	√	I	Eqs. (7), (8)	–	Eqs. (140)–(142)
								III	Eqs. (12), (143)–(145)		
[39]	I	PCP model (Diffusion in the radial direction of a particle)						I	Eqs. (153), (156)	W T_s	Eqs. (36), (126)–(128), (158)–(161)
								III	Eqs. (154)		
[40]	I	PCP model						II	Eqs. (166), (167)	W H_g H_d Y_a	Eqs. (162), (164), (165)

the desiccant wheel. To solve this problem, models considering heat and mass transfer in both solid and air side are proposed. Such models are called GSSR models (listed in Table 3). GSSR model is more preferable compared with GSR model for it can explain the effect of heat and mass diffusion within solid desiccant and the precision of governing equations describing the physics of desiccant wheel is enhanced.

Typical diffusion theory holds that water vapor molecule has three types of diffusion mode in porous mediums which includes: ordinary diffusion, Knudson diffusion and surface diffusion. The actual diffusion process is the combination of these three mechanisms.

Ordinary diffusion which is also called molecular diffusion or Fickian diffusion occurs when the mean free path is relatively short compared to the pore size. This diffusion mode is applicable to Brownian motion, where the movement of each particle is random and not dependent on its previous motion. The transfer diffusivity D_O relates the macroscopic flux of molecules in a system to a driving force in the concentration. Knudson diffusion occurs when the mean free path of gas molecules is relatively long compared to the pore size. It describes situations in which gas molecules collide more frequently with flow boundaries than with other gas molecules. Knudsen diffusion is dominant for pores that range in diameter between 2 and 50 nm. Surface diffusion is also used to explain a type of pore diffusion in which solutes adsorb on the surface of the pore and hop from one site to another through interactions between the surface and molecules. All of these transport processes can be described by means of Fick's law of diffusion with appropriate diffusion coefficients (D_O, D_K, D_S).

Pesaran and Mills [39] investigated the diffusion mechanism in silica gel. It has been reported that surface diffusion is the dominant one for moisture transfer in micro porous silica gel such as RD gel (regular density silica gel). While for macro porous silica gel, for example ID gel (intermediate density silica gel), both Knudsen and surface diffusions are important mechanism. Ordinary diffusion can be negligible for the silica gel at atmospheric pressure.

Based on different methods to account for the SSR, GSSR models are classified into three subcategories: (i) pseudo-gas-side (PGS) models in which lumped convective coefficients are adopted to account for SSR; (ii) gas and solid-side (GSS) models in which the second order diffusion terms are added to account for SSR; (iii) parabolic concentration profile (PCP) models which assume that a parabolic concentration profile for moist concentration exists at all the times in the desiccant particle.

4.1. Pseudo-gas-side (PGS) model

A simplified method to include the heat and mass transfer in the solid desiccant is using lumped transfer coefficients (h' as heat transfer coefficient and K'_y as mass transfer coefficient) which include heat and mass transfer resistances not only in gas side but also in solid side. Such modified models are named as PGS model. Since the second-order diffusion terms are not added, the complexity and computational time of PGS model do not increase compared with GSR model. The lumped transfer coefficients are usually obtained by the correlations of experimental data. The correlations for silica gel as adsorbent given by the Hougen and Marshall [41] based on Ahlberg's experimental

data [42] are in wide use:

$$h' = 0.683 m_i' \,\mathrm{Re}^{-0.51} c_{pa}, \tag{69}$$

$$K_y' = 0.704 m_i' \,\mathrm{Re}^{-0.51}. \tag{70}$$

4.1.1. Axial-flow PGS model

Maclaine-Cross [43] has presented a finite-difference model known as MOSHMX (method of solving heat and mass exchangers). The gas-side controlled, lumped capacitance mass transfer coefficient was used in the model which is actually a typical PGS model. A model of desiccant wheel with PGS coefficients similar to the one proposed by Maclaine-Cross [43] has been described by Holmberg [32]. In the model, air thermal and moisture storage capacities $\partial Y/\partial t$ and $\partial T/\partial t$ were neglected due to their small value compared to the matrix capacities. The control volume is depicted in Fig. 7.

Mass and energy conservation equations were:

$$\dot{m}_a \frac{\partial Y_a}{\partial z} + \frac{f m_m}{L}\frac{\partial W}{\partial t} = 0, \tag{71}$$

$$\dot{m}_a \frac{\partial H_a}{\partial z} + \left(\frac{m_m}{L}\frac{\partial H_m}{\partial t} - kA_m \frac{\partial^2 T_m}{\partial z^2}\right) = 0. \tag{72}$$

Mass and energy transfer equations were:

$$\dot{m}_a \frac{\partial Y_a}{\partial z} = \frac{K_y' m_m}{L}(Y_m - Y_a), \tag{73}$$

$$\dot{m}_a \frac{\partial H_a}{\partial z} = \frac{K_y' A}{L}\left[\frac{h'}{K_y'}(T_m - T_a) + h_{fg}(Y_m - Y_a)\right], \tag{74}$$

where it is assumed that the rotor matrix is composed of supporters (*sp*) and adsorbent (*d*) with the mass fractions $1-f$ and f, respectively. Thus the enthalpy of the matrix is defined by

$$H_m = (1-f)H_{sp} + f[H_d + W(H_{ws} - q_{st} + h_{fg})]. \tag{75}$$

The equilibrium isotherm was in the form of Eq. (18)

$$W = 0.55\Phi. \tag{76}$$

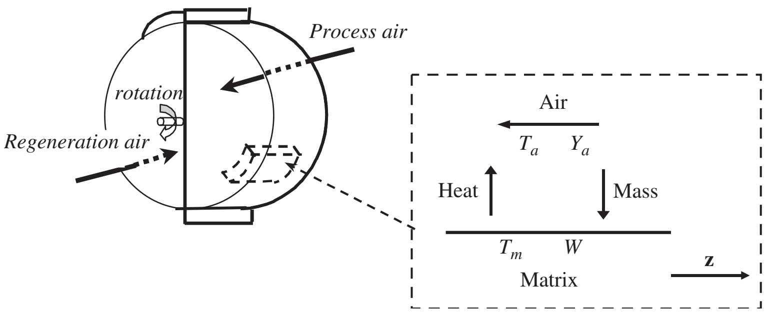


Fig. 7. The model of control volume and a side view of one of ducts for axial-flow PGS model [32].

Holmberg adopted implicit Crank–Nicholson scheme for the energy conservation equation (72) and ordinary central difference schemes for other equations. Gauss–Seidel solution technique was employed to solve the model. A parametric study was conducted to show the influences of matrix heat and moisture capacities on temperature and humidity efficiencies. It was indicated that there is an optimum drying humidity efficiency with variable heat capacities and the optimum value increases in magnitude with increasing moisture capacity.

Based on the studies of Maclaine-Cross [43] and Holmberg [32], Jurinak and Mitchell [9] neglected the axial heat conduction inside the matrix and developed a dimensionless PGS model in period j (j is a period index) of rotary dehumidifier. The control volume was the same as shown in Fig. 7 and the governing equations were given as:

Mass and energy conservation in period j:

$$\frac{\partial Y_a}{\partial z'} + \theta_j'(\mu k)_j \frac{\partial W}{\partial \theta'} = 0, \tag{77}$$

$$\frac{\partial H_g}{\partial z'} + \theta_j'(\mu k)_j \frac{\partial H_m}{\partial \theta'} = 0, \tag{78}$$

where coefficients μ_j and κ_j are defined as:

$$\mu_j = m_{\text{dry matrix mass}, j}/m_{\text{dry air containned in matrix}, j} \quad k_j = L/(\mu_j \theta_j). \tag{79}$$

Mass and heat transfer equations in period j:

$$\frac{\partial Y_a}{\partial z'} = \Lambda_{w,j}(Y_m - Y_a), \tag{80}$$

$$\frac{\partial H_g}{\partial z'} = \Lambda_{w,j}(Le_o c_{pg}(T_m - T_a) + H_v(Y_m - Y_a)), \tag{81}$$

where dimensionless coordinates in the governing equations are

$$z' = z/L, \quad \theta' = \theta/t_r, \quad \theta_j' = \theta_j/t_r \tag{82}$$

and dimensionless heat and mass transfer length are given by

$$\Lambda_{T,j} = J_{T,j}L/v_j, \quad J_{T,j} = \frac{4h'}{\rho_a d_e c_{pg}}, \tag{83}$$

$$\Lambda_{w,j} = J_{w,j}L/v_j, \quad J_{w,j} = \frac{4K_y'}{\rho_a d_e}. \tag{84}$$

Overall Lewis number was expressed as

$$Le_0 = J_{T,j}/J_{w,j}. \tag{85}$$

The enthalpy of the matrix at any temperature and water content with respect to a dry matrix at 273 K were given by

$$H_m = c_{pm}(T_m - 273) + c_{pl}W(T_m - 273) + h_{fg}\int_0^W (1 - h^*)\,\mathrm{d}W, \tag{86}$$

$$\frac{q_{st}}{h_{fg}} = h^*(W/W_{\max}) = 1 + \Delta h^* \frac{\exp(\lambda W/W_{\max}) - \exp(\lambda)}{1 - \exp(\lambda)}, \quad \lambda = \text{constant}, \tag{28}$$

where the dry matrix thermal capacities, c_{pm}, is related to the specific heat of desiccant c_{pd} and of the nonsorbing matrix materials c_{pi}

$$c_{pm} = c_{pd} + \sum_i (m_i c_{pi})/f. \tag{87}$$

Six different isotherm equations were adopted in the study to investigate their influences. They are functions of $W/W_{\max}$ and here only the simplest linear style is listed in detail:

$$\Phi = G(W/W_{\max}) = W/W_{\max}. \tag{88}$$

A finite difference solution was used to study the effects of different matrix properties on the performance of a rotary dehumidifier, and in each case the results were obtained for the maximum dehumidification efficiency. The results were useful to select desiccant and analyze the open-cycle systems.

Cejudo et al. [44] validated the model proposed by Jurinak and Mitchell [9] by experimental data. Moreover, they used the real data to train a neural network to calculate the parameters of a new neural network model. Their results demonstrated that the new neural network model is more adequate to simulate wheel performance when heat losses of the rotating wheel are taken into account.

Later, Van den Bulck et al. [33] pointed out that, the model solution in Ref. [9] involved considerable computation and was not suitable for long-term simulation of desiccant cooling systems. In order to reduce the calculation efforts, they introduced number of transfer units (NTU) in the governing equations. The new conservation equations using NTU for period j were

$$\frac{\partial Y_a}{\partial z'} + \frac{\partial W}{\partial t'} = 0, \tag{89}$$

$$\frac{\partial H_g}{\partial z'} + \frac{\partial H_m}{\partial t'} = 0, \tag{90}$$

$$\frac{\partial Y_a}{\partial z'} = \mathrm{NTU}_{w,j}(Y_m - Y_a), \tag{91}$$

$$\frac{\partial H_g}{\partial z'} = \mathrm{NTU}_{t,j}\frac{\partial H_g}{\partial T_g}(T_m - T_a) + \mathrm{NTU}_{w,j} H_v (Y_m - Y_a), \tag{92}$$

where air stream mass flow rates, wheel rotation speed and mass of desiccant are combined into two dimensionless capacitance rate parameters Γ_j:

$$\Gamma_j = \frac{m_d}{t_r \dot{m}_j} \quad (j = 1, 2), \quad t' = \frac{\theta}{\theta_j}\frac{1}{\Gamma_j} \quad \left(0 \leqslant t' \leqslant \frac{1}{\Gamma_j}\right), \quad z' = z/L \tag{93}$$

and the number of transfer units is defined as

$$\mathrm{NTU}_{w,j} = \frac{K'_y A_j}{\dot{m}_j}, \tag{94}$$

$$\mathrm{NTU}_{t,j} = \frac{h' A_j}{\dot{m}_j c_{pg}}, \quad c_{pg} = \left(\frac{\partial H_g}{\partial T_g}\right)_{\bar{Y}_a}. \tag{95}$$

This approach is called effectiveness-number of transfer units (ε-NTU) method which clearly represents the influence of flow unbalance and transfer coefficients respectively. Boundary conditions in mode II and thermophysical property parameters obtained from Ref. [45] were applied to close the partial difference equations. Then the model was solved by means of characteristics and the shock wave method. Using this model, the performance correlation of ideal dehumidifier with infinite heat and mass transfer coefficients was calculated as a function of NTU and operating parameters Γ_j.

Subsequently, correlations for the humidity and enthalpy effectiveness of actual silica gel dehumidifiers with finite transfer coefficients as functions of NTU were conducted by Van den Bulck et al. [46]. In their analysis, equilibrium isotherm and enthalpies of gas and matrix were calculated by

$$\Phi = (2.112W)^{q_{st}/h_{fg}}(29.91P_{vs})^{q_{st}/h_{fg}-1}, \tag{96}$$

$$H_g = c_{pg}(T_g - T_{\text{ref}}) + H_v[T_{\text{ref}}]Y_g, \tag{97}$$

$$H_m = c_{pd}(T_d - T_{\text{ref}}) + \int_0^{\text{W}} (H_v[T_{\text{ref}}] - q_{st}[\Omega, T_{\text{ref}}])\, \mathrm{d}\Omega. \tag{98}$$

The correlations were validated by comparing the effectiveness values obtained from these correlations with effectiveness values provided by MOSHMX [43] and the ideal dehumidifier theory [33]. The results showed that a ε-NTU model incorporating these correlations can rapidly and accurately predict the dehumidifier performance. And they were suitable to be used in long term performance simulation of desiccant cooling system.

Also, by using the same ε-NTU model, Klein et al. [1] analyzed a regenerative enthalpy exchanger, Van den Bulck et al. [47] investigated a desiccant cooling system and a modified method was proposed to solve ε-NTU model for the desiccant which has discontinuous isotherms and isopiestics such as LiCl [48].

4.1.2. Radial-flow PGS model

The one-dimensional desiccant wheels focused on axial flow have been extensively investigated in the literatures as described in previous section. Elsayed and Chamkha [34] studied the radial flow desiccant wheel and developed a model to predict its performance. The radial flow wheel with an inner radius r_1 and outer radius r_2 is shown in Fig. 8. It is

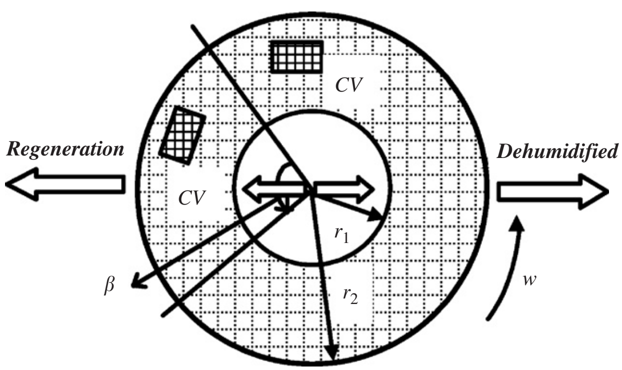


Fig. 8. Schematic of radial-flow desiccant wheel and the model of control volume for radial-flow PGS model [34].

divided into two sections: period 1 of fraction β for regeneration air and period 2 of fraction $1-\beta$ for process air. The air flows in the radial direction inwards or outwards. The assumptions for the model were similar to that of Jurinak and Mitchell [9] and Van den Bulck et al. [46].

Conservation of moisture in the air was expressed by

$$\dot{m}_i \frac{\mathrm{d}A_i}{A_i}\frac{\partial Y_a}{\partial r}\,\mathrm{d}r = K'_y A_V\,\mathrm{d}A_i\,\mathrm{d}r(Y_m - Y_a). \tag{99}$$

Conservation of moisture in the matrix was given by

$$m_m\omega\frac{2\pi r\mathrm{d}r}{\pi(r_2^2-r_1^2)}\frac{\partial \mathrm{W}}{\partial t}\,\mathrm{d}t = K'_y A_V\,\mathrm{d}A_i\,\mathrm{d}r(Y_a - Y_m). \tag{100}$$

Conservation of energy in the air yielded

$$\dot{m}_i \frac{\mathrm{d}A_i}{A_i}\frac{\partial H_g}{\partial r}\,\mathrm{d}r + K'_y A_V\,\mathrm{d}A_i\,\mathrm{d}rH_v(Y_m - Y_a) = hA_V\,\mathrm{d}A_i\,\mathrm{d}r(T_m - T_a). \tag{101}$$

Conservation of energy in the matrix yielded

$$m_m\omega\frac{2\pi r\mathrm{d}r}{\pi(r_2^2-r_1^2)}\frac{\partial H_m}{\partial t}\,\mathrm{d}t + \dot{m}_i\frac{\mathrm{d}A_i}{A_i}\frac{\partial H_g}{\partial r}\,\mathrm{d}r = 0. \tag{102}$$

The boundary conditions in modes I and II were applied in the model. Periodic boundary condition was expressed by the following equations:

$$W(r/r_1, \omega\mathrm{t} = 0) = W(r/r_1, \omega\mathrm{t} = 1), \tag{103}$$

$$T_m(r/r_1, \omega\mathrm{t} = 0) = T_m(r/r_1, \omega\mathrm{t} = 1). \tag{104}$$

Based on experimental data, the corrected compound heat and mass transfer coefficients h' and K' were dependent on the superficial air velocity u within a matrix cross-sectional area [49]

$$h' = C_h u^a, \tag{105}$$

$$K'_y = C_m u^a \rho_a, \tag{106}$$

where C_h, C_m and α are constants.

The relations to determine the heat of sorption, equilibrium humidity ratio of air in contact with a silica gel matrix and the enthalpy of the silica gel were the same as Eqs. (35), (96)–(98).

These differential governing equations were reduced to dimensionless NTU style and discretized by finite difference technique on staggered grid. Parametric studies were performed using the model to determine the effects of flow configuration and operational parameters on the performance of radial flow silica gel desiccant wheel were studied. Also axial flow desiccant wheel was compared with conventional radial flow wheel. It was founded that whose performance is better depending on the values of the design and operating parameters. For instance, in ventilation and recirculation modes, a radial flow wheel with $\alpha = 2$ (Eq. (105)) has lower outlet humidity ratio of process air and higher performance coefficient than axial flow wheel. But when $\alpha \geqslant 6$, the results are opposite.

It should be noted that composite transfer coefficients h' and K'_y are used to account for solid diffusion resistance in PGS models. Therefore, although second-order differential

terms are not added in the governing equations and the style of the equation is almost the same as GSR model. The SSRs are indirectly included. That is why PGS model is excluded from GSR model and included in GSSR model.

Since the composite coefficients are obtained from large numbers of experimental results, it is not convenient for studying a variety of desiccant materials and geometries. And by now, only the data for silica gel has been obtained. Hence, the reliance on such excessive available data limits the application of PGS model. Besides, the reliability of PGS model is not good enough which hinders its further development. Clark et al. [50] tested a prototype bed designed for solar air conditioning and found the results were in rather poor agreement with predictions based on the PGS model, particularly after a step change in inlet air condition. They concluded that the discrepancy was due to the shortcomings of the model, since the SSR exceeds the GSR under these conditions. The experimental result reported by Clark et al. [50] was somewhat limited and imprecise for the bed with a large prototype design. Hence Pesaran [21] performed bench scale experiments on thin beds of regular density silica gel with step changes in inlet air humidity. Their results conformed that the SSR was indeed generally larger than GSR. Also, the results of Mei and Lavan [51] indicated that the predicted results obtained from PGS model were acceptable compared with experiment results, but the coherence was not very well. Furthermore, Gheelayagh and Gidaspow [52] pointed out that the composite coefficients h' and K'_y that represent the SSRs were not constant, their value changed with the time. So adopting constant composite coefficients cannot reliably forecast the performance of dehumidifier.

4.2. Gas and solid-side (GSS) model

Since PGS models adopting lumped transfer coefficients cannot provide very accurate results, and there exists a demand for suitable models containing SSRs. With the increasing knowledge of diffusion mechanism inside desiccant, gas and solid-side (GSS) models are proposed in which heat and mass transfer diffusional terms in solid-side are directly added. Although GSS model needs more time to compute the additional second order diffusion terms compared with PGS model, it is more related to the true physics of the problem. Therefore, GSS model is likely to give better agreement with experiment results.

4.2.1. One-dimensional model

Using the control volume illustrated in Fig. 9, San and Hsiau [35] have derived a one-dimensional model considering the axial mass diffusion and heat conduction in solid

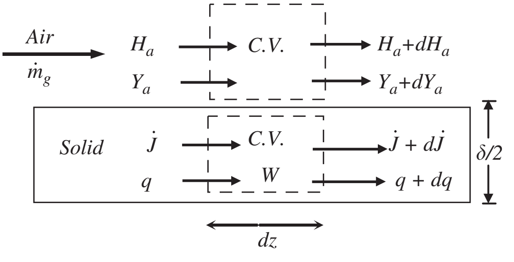


Fig. 9. The model of control volume for a one-dimensional GSS model [35].

desiccant, while the storage terms of moisture and energy in air $\partial Y_a/\partial t$ and $\partial T_a/\partial t$ were neglected. The mass and energy balances were expressed as:

Conservation of moisture in air:

$$\dot{m}_a \frac{\partial Y_a}{\partial z} = \frac{A_V V}{2L} K_y (Y_m - Y_a). \tag{107}$$

Conservation of moisture in solid:

$$m_m f \frac{\partial W}{\partial t} - A_V V \frac{\delta}{2} D_S \frac{\partial^2 W}{\partial z^2} = A_V V K_y (Y_a - Y_m), \tag{108}$$

where the surface diffusivity is evaluated by

$$D_S = \frac{1.6 \times 10^{-6} \rho_m}{\tau} \exp\left(-0.974 \times 10^{-6} \times \frac{q_{st}}{T_m}\right). \tag{109}$$

Conservation of energy in air:

$$c_{pg} \dot{m}_g \frac{\partial T_a}{\partial z} = \frac{A_V V}{2L} h (T_m - T_a). \tag{110}$$

Conservation of energy in solid:

$$m_m c_{pm} \frac{\partial T_m}{\partial t} - A_V V \frac{\delta}{2} k \frac{\partial^2 T_m}{\partial z^2} = A_V V h (T_a - T_m) + A_V V K_y (Y_a - Y_m) q_{st}, \tag{111}$$

where k is the compound conduction coefficient and calculated using the following expression:

$$k = f \cdot k_d + (1 - f) k_{sp} \tag{112}$$

and subscript "m" means the solid part of the wheel which contains desiccant and substrate materials and then "m_m" stands for the total mass of solid desiccant wheel.

RD gel was selected as desiccant in the study. Due to surface diffusion is the only mechanism need to be considered for RD gel [39], only "D_S" which represents surface mass diffusion coefficient appears in the model. The heat of sorption and equilibrium isotherm relationship were determined by Eqs. (35) and (96). The saturation pressure of vapor P_{vs} was evaluated using the following expressions:

$$\log_{10} \frac{P_{vs}}{218.167} = -\frac{z}{T} \frac{a + bz + cz^3}{1 + dz}, \tag{113}$$

$$\begin{cases} z = 100.97 - \mathrm{T}; \;\; a = 3.2437814; \;\; b = 5.86826 \times 10^{-3}, \\ c = 1.1702379 \times 10^{-8}; \;\; d = 2.1878463 \times 10^{-3}. \end{cases}$$

The relationship between Y_m, T_m and Φ was obtained from ASHRAE data

$$Y_m = \frac{6.22 \times 10^{-3} \Phi}{10^{4.21429 - [7.5(T_m - 273.15)/(T_m - 35.85)]} - \Phi/100}. \tag{114}$$

A mixed numerical scheme was developed to solve the governing equations. The two governing equations in desiccant side (Eqs. (108) and (111)) were solved using full-implicit finite difference scheme and the other two in gas side (Eqs. (107) and (110)) were solved using backward finite difference scheme. The full-implicit finite-difference scheme was

verified to be effective for solving the equation with diffusion terms. Also this mixed scheme was compared with the explicit scheme which solved the four governing equations totally with a backward finite difference scheme. It showed that for the same accuracy the mixed scheme takes less computation time than the explicit scheme. On the other hand, for the same time step Δt the balance in the mixed scheme is much better than that in the explicit scheme.

Numerical results of this model indicated that the axial heat and mass diffusion are governed by two important parameters NTU and $\delta^2/4Bi$, and for a case of zero SSR, the calculated performance of the silica-gel desiccant wheel is poor. Furthermore, it was found that only taking account of surface diffusion is good enough for predicting RD silica gels desiccant wheel, but for ID silica gels the Knudsen and ordinary diffusion are needed to be considered.

4.2.2. Two-dimensional model

Charoensupaya and Worek [10] established a two-dimensional GSS model in which the heat conduction and mass diffusion including gas phase diffusion and surface diffusion in the radial direction within solid desiccant were considered. The control volume is illustrated in Fig. 10.

Conservation of moisture in the process air was expressed as

$$\frac{\dot{m}_a}{X_m}\left(\frac{1}{u}\frac{\partial Y_a}{\partial t}+\frac{\partial Y_a}{\partial z}\right)=2K_y(Y_d-Y_a). \tag{115}$$

Conservation of moisture in the desiccant felt was given by

$$\varepsilon_t\rho_{ad}\frac{\partial Y_d}{\partial t}+(1-\varepsilon_t)\rho_d\frac{\partial W}{\partial t}-D_G\rho_{ad}\frac{\partial^2 Y_d}{\partial r^2}-D_S\rho_d\frac{\partial^2 W}{\partial r^2}=0, \tag{116}$$

where D_G and D_S represent the effective gas phase diffusivity and surface diffusivity, respectively.

Conservation of energy within the desiccant felt gave

$$\varepsilon_t\rho_{ad}\frac{\partial H_{ad}}{\partial t}+(1-\varepsilon_t)\rho_d c_{pd}\frac{\partial T_d}{\partial t}-k_d\frac{\partial^2 T_d}{\partial r^2}=(1-\varepsilon_t)\rho_d q_{st}\frac{\partial W}{\partial t}, \tag{117}$$

where the subscript "*ad*" means the air in desiccant pore.

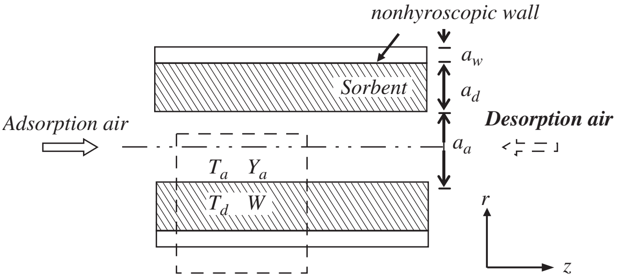


Fig. 10. The model of control volume for a two-dimensional GSS model [10].

The rate of energy transfer between process air and desiccant felt yielded

$$\frac{\partial H_g}{\partial t}+u\frac{\partial H_g}{\partial z}=\frac{2K_y}{\rho_g\alpha_a}(Y_d(t,x,\alpha_d)-Y_a)\frac{\partial H_g}{\partial Y_a}+\frac{2h}{\rho_g\alpha_a}(T_d(t,x,\alpha_d)-T_a). \tag{118}$$

The boundary conditions were in the form of mode III. Also, the temperature of the wall was assumed to be the same as the desiccant temperature at $r=0$

$$T_w(t,z)=T_d(t,z,0). \tag{119}$$

The model was verified using the following equilibrium relation and heat of sorption:

$$W=0.5\Phi, \tag{120}$$

$$q_{st}=h_{fg}. \tag{121}$$

The heat and mass transfer coefficients were approximately by constant value that can be calculated from the Nusselt and Sherwood number correlations.

An explicit finite-difference scheme was adopted as the solution method to calculate the model. The model was used to analyze the effect of some parameters, including heat and mass transfer Biot number, on the performance of desiccant cooling system. It was revealed that there exist optimum values of COP and cooling capacity for given operating conditions. The optimum values can be reached by controlling the system cycle time. Also the accuracy of this model has been verified by experimental data in Ref. [53].

Yu et al. [36,54] also constructed a two-dimensional mathematical model for desiccant wheel based on the control volume shown in Fig. 2. Both the mass diffusion and heat conduction inside the solid desiccant wheel in axial as well as circumferential directions were considered in the model. The governing equations are listed as follows:

Conservation of moisture in the air:

$$\frac{\partial Y_a}{\partial t}+\omega\frac{\partial Y_a}{\partial\varphi}+\frac{m_i'}{\rho_iF_s}\frac{\partial Y_a}{\partial z}=\frac{K_yA_V}{\rho_iF_s}(Y_d-Y_a). \tag{122}$$

Conservation of moisture in solid adsorbent:

$$\frac{\partial W}{\partial t}+\omega\frac{\partial W}{\partial\varphi}-D_e(1-F_s)\left[\frac{2\ln(r_2/r_1)}{r_2^2-r_1^2}\frac{\partial^2 W}{\partial\varphi^2}+\frac{\partial^2 W}{\partial z^2}\right]=\frac{K_yA_V}{\rho_d}(Y_a-Y_d). \tag{123}$$

Conservation of energy in the air:

$$\frac{\partial T_a}{\partial t}+\omega\frac{\partial T_a}{\partial\varphi}+\frac{m_i'}{\rho_iF_s}\frac{\partial T_a}{\partial z}=\frac{hA_V}{\rho_iF_s(c_{pa}+Y_ac_{pv})}(T_d-T_a). \tag{124}$$

Conservation of energy in solid desiccant:

$$\begin{aligned}&\frac{\partial T_d}{\partial t}+\omega\frac{\partial T_d}{\partial\varphi}-\frac{k_d(1-F_s)}{[\rho_d(c_{pd}+Wc_{pl})+\rho_{sp}c_{psp}]}\left[\frac{2\ln(r_2/r_1)}{r_2^2-r_1^2}\frac{\partial^2 T_d}{\partial\varphi^2}+\frac{\partial^2 T_d}{\partial z^2}\right]\\&\quad=\frac{[hA_V(T_a-T_d)+K_yA_V(Y_a-Y_d)q_{st}]}{[\rho_d(c_{pd}+Wc_{pl})+\rho_{sp}c_{psp}]}.\end{aligned} \tag{125}$$

The boundary and initial conditions were similar to those of Ref. [14]. Eq. (26) was adopted to calculate Y_d. Equilibrium isotherms Φ, obtained by fitting fourth-degree

polynomials to the manufacture data [21], and heat of sorption q_{st} for RD and ID were:

For RD gel:

$$\Phi = 0.0078 - 0.05759W + 24.16554W^2 - 124.478W^3 + 204.226W^4, \tag{36}$$

$$q_{st} = \begin{cases} -12400W + 3500 & W \leqslant 0.05 \ \text{(kJ/kg water)}, \\ -1400W + 2950 & W > 0.05 \ \text{(kJ/kg water)}, \end{cases} \tag{126}$$

For ID gel:

$$\Phi = \begin{cases} 1.235W + 267.99W^2 - 3170.7W^3 + 10087.16W^4 & \text{W} \leqslant 0.07, \\ 0.3316 + 3.18W & \text{W} > 0.07, \end{cases} \tag{127}$$

$$q_{st} = \begin{cases} -300\text{W} + 2095 & \text{W} \leqslant 0.15 \ \text{(kJ/kg water)}, \\ 2050 & \text{W} > 0.15 \ \text{(kJ/kg water)}. \end{cases} \tag{128}$$

Central difference scheme was applied to discretize the diffusion items and the same schemes as in Ref. [8] were adopted to discretize the other terms. It was demonstrated the numerical results of this model are very close to the steady and transient experimental data of Refs. [55,56].

Dai et al. [57] pointed out that the model proposed by Yu et al. [36] was helpful for predicting the performance of desiccant wheel but was not brief enough. Hence they adopted psychrometric wave chart analysis associated with the finite difference model trying to obtain the numerical results efficiently. In their study, RD silica gel was used as adsorbent. According to the conclusion of Pesaran [39], the surface diffusion is dominant for RD silica gel, and then the effective diffusivity was given as

$$D_e = D_S = D_0 \exp\left(-0.974 \times 10^{-6} \times \frac{q_{st}}{T_d}\right), \quad D_0 = 0.8 \times 10^{-6}. \tag{129}$$

Using the wave analysis in psychrometric chart incorporating with numerical calculation, the influences of some important parameters, such as heat capacity, adsorption heat, rotation speed, thickness of the desiccant matrix, etc., on the performance of RD silica gel desiccant wheel system were discussed. It was found that the chart method is rapid in evaluating the system performance and is useful in system design.

Gao et al. [58] have described a mathematical model that can be seen as the simplification form proposed by Yu [36], where diffusion terms in circumferential direction were ignored and the sensible heat transfer was included in the governing equations. They conducted a parameter analysis employing the model to investigate the effects of passage shape and geometrical size of the matrix on the performance of desiccant wheel.

Zhang and Niu [37] have presented a two-dimensional transient model in which heat conduction, surface and gaseous diffusion in axial as well as radial directions of the desiccant wheel are included simultaneously. Due to symmetry, the mid-plane of a channel was treated as adiabatic wall, and a half-size channel was chosen as the control volume as shown in Fig. 11. The derived governing equations were:

Conservation of moisture in the air stream:

$$\frac{1}{u}\frac{\partial Y_a}{\partial t} + \frac{\partial Y_a}{\partial z} = \frac{4K_y}{d_e u \rho_g}(Y_s - Y_a). \tag{130}$$

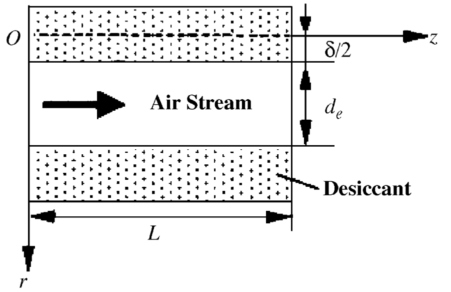


Fig. 11. The model of control volume for a two-dimensional GSS model [37].

Conservation of moisture in the desiccant:

$$\varepsilon_t \rho_{ad} \frac{\partial Y_d}{\partial t} + \rho_d \frac{\partial W}{\partial t} = \rho_{ad} \left[\frac{\partial}{\partial z} \left(D_G \frac{\partial Y_d}{\partial z} \right) + \frac{\partial}{\partial r} \left(D_G \frac{\partial Y_d}{\partial r} \right) \right] + \rho_d \left[\frac{\partial}{\partial z} \left(D_S \frac{\partial W}{\partial z} \right) + \frac{\partial}{\partial r} \left(D_S \frac{\partial W}{\partial r} \right) \right], \tag{131}$$

where the effective surface diffusivity D_S can be calculated by Eq. (129) and D_G which stands for the composite effective diffusivity of Kundsen and ordinary diffusion is given by

$$D_G = \frac{\varepsilon_t}{\tau} \left(\frac{1}{D_O} + \frac{1}{D_K} \right)^{-1}, \quad D_O = 1.758 \times 10^{-4} \frac{T_d^{1.685}}{B}, \quad D_K = 97a \left(\frac{T_d}{m_1} \right)^{0.5}, \tag{132}$$

where a (m) is the pore radius of the adsorbent and m_1 (kg/mol) is the molecule weight of water.

Conservation of energy in the air stream:

$$\frac{1}{u} \frac{\partial T_a}{\partial t} + \frac{\partial T_a}{\partial z} = \frac{4h}{d_e u \rho_g c_{pg}} (T_s - T_a). \tag{133}$$

Conservation of energy in the desiccant:

$$\rho_d c_{pt} \frac{\partial T_d}{\partial t} = k_d \left(\frac{\partial^2 T_d}{\partial z^2} + \frac{\partial^2 T_d}{\partial r^2} \right) + q_{st} \rho_d \frac{\partial W}{\partial t}, \tag{134}$$

where c_{pt} is the total heat capacity of wet desiccant, which included two parts: dry desiccant and adsorbed water and is calculated by

$$c_{pt} = c_{pd} + W c_{pl}. \tag{135}$$

By using heat mass transfer analogy, the relations between h and K_y can be expressed as

$$K_y = \frac{h}{c_{pg} Le}. \tag{136}$$

Water content in the desiccant is governed by a general sorption isotherm as

$$W = \frac{f W_{\max}}{1 - R + R/\Phi} \tag{137}$$

The boundary conditions were similar to Eqs. (5)–(8), (12), (14). This model was normalized and numerically solved by means of alternating direction implicit (ADI)

method [59]. Using the model, effects of rotary speed, NTU and specific area on the performance of silica gel wheel were studied and compared in desiccant wheels for dehumidification and enthalpy recovery.

Niu and Zhang [60] performed an analysis study adopting the above model to study the influence of wall thickness on the optimum rotary speeds for dehumidification desiccant wheel and enthalpy recovery wheel.

Sphaier and Worek [38] derived a desiccant wheel mathematical model which accounts for heat and mass transfer processes inside solid desiccant too. The model is different from others in two aspects: (1) the diffusion terms in the governing equations are given in the form of vector, hence governing equations can be easily converted into one or two, even three-dimensional ones; (2) parameters describing detailed constitution of felt are included in the model. The model is thought to be useful for analyzing the transport phenomena within the porous adsorbent felt and the influence of supporting structure. It is assumed that the entire felt (subscript "*f*") is composed of rigid matrix (subscript "*fm*") and pores (subscript "*fp*") in which both the gas and adsorbed liquid phase coexist. The matrix includes solid adsorbent desiccant (subscript "*fd*") and inert materials which has no effects on the sorption characteristics of adsorbent and surface diffusion.

Based on the control volume shown in Fig. 12, the derived conservation equations of moisture and energy in the air stream were similar to Eqs. (130), (133), and conservation equations of moisture and energy in the desiccant were:

$$\varepsilon_t \rho_a \frac{\partial Y_{fp}}{\partial t} + (1-\varepsilon_t)\rho_{fd} f \frac{\partial W_{fm}}{\partial t} = \rho_a \nabla(D_{G,\mathrm{eff}} \nabla Y_{fp}) + \rho_{fs} f \nabla(D_{\mathrm{S,eff}} \nabla W_{fm}), \tag{138}$$

$$\rho_f c_f \frac{\partial T_f}{\partial t} = \nabla(k_{f,\mathrm{eff}} \nabla T_f) + \rho_{fd} f \left[(1-\varepsilon_t)\frac{\partial W_{fm}}{\partial t} - \nabla(D_{\mathrm{S,eff}} \nabla W_{fm})\right] q_{st}, \tag{139}$$

where the effective heat conductivity $k_{f,\mathrm{eff}}$ gas phase and surface diffusivity $D_{G,\mathrm{eff}}$, $D_{S,\mathrm{eff}}$ are defined as

$$k_{f,\mathrm{eff}} = \varepsilon_t k_{fp} + (1-\varepsilon_t) k_{fm}, \tag{140}$$

$$D_{G,\mathrm{eff}} = \varepsilon_t D_G / \tau_g, \tag{141}$$

$$D_{\mathrm{S,eff}} = (1-\varepsilon_t) D_{\mathrm{S}} / \tau_s. \tag{142}$$

Eqs. (7) and (8) were utilized to depict the insulated and impermeable boundaries. Boundary conditions in mode III were obtained through interface balances: at $r = R_g$ (Fig. 12), the boundary condition for mass transport was the same as Eq. (12) and for heat

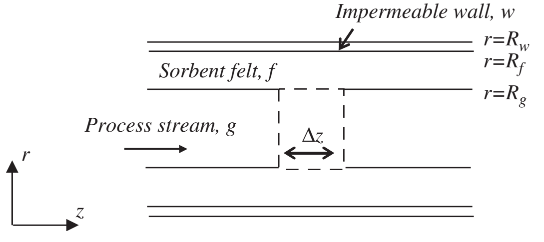


Fig. 12. The model of control volume for a GSS model with vector form [38].

transport was given as:

$$-k_{f,\text{eff}}\frac{\partial T_f}{\partial r} = h(T_a - T_f) + K_y(Y_a - Y_{fp})q_{\Delta T} - \rho_{fd}D_{\text{S,eff}}\frac{\partial W_{fm}}{\partial r}q_{st} \tag{143}$$

and at the wall the boundary conditions were

$$-\rho_a D_{G,\text{eff}}\frac{\partial Y_{fp}}{\partial r} - \rho_{fd}D_{\text{S,eff}}\frac{\partial W_{fm}}{\partial r} = 0, \tag{144}$$

$$\dot{q}_s = -k_{f,\text{eff}}\frac{\partial T_f}{\partial r} - \rho_a D_{G,\text{eff}}\frac{\partial Y_{fp}}{\partial r}q_{\Delta T} - \rho_{fd}D_{\text{S,eff}}\frac{\partial W_{fm}}{\partial r}H_l, \tag{145}$$

where $q_{\Delta T}$ is termed the heat of sorbate transfer at the interface

$$q_{\Delta T} = c_{pv}(T_a - T_d). \tag{146}$$

Also the selecting equilibrium isotherm was in the form of Eq. (17).

These governing equations were fully normalized using classical dimensionless groups for heat and mass transfer, and a numerical algorithm based upon the finite volumes method was employed to solve it. It showed that simulation results present a very reasonable agreement with the experimental data. Moreover the simulation results of a test-case were presented, suggesting a possible optimization to wheel initial-cost and compactness by reducing felt thickness. This model can be applied for the simulation of several configurations such as desiccant wheels or enthalpy exchangers.

4.3. Parabolic concentration profile (PCP) model

Pseudo-gas-side (PGS) model and gas and solid-side (GSS) model have their own shortcomings. The GSS model requires greater computational effort than PGS model because of the additional second-order heat and mass transfer diffusional items. However, the PGS model requires extensive experimental data for determination of the lumped transfer coefficients with different desiccant materials and its reliability is not good enough. Hence, a computationally efficient model that effectively considers both the SSRs and GSRs in desiccant wheel is needed. Parabolic concentration profile (PCP) model assuming an analytically convection concentration profile within the desiccant particle to account for solid-side diffusion is developed to achieve this objective. Usually, based on the assumed concentration profile, a differential governing equation describing mass

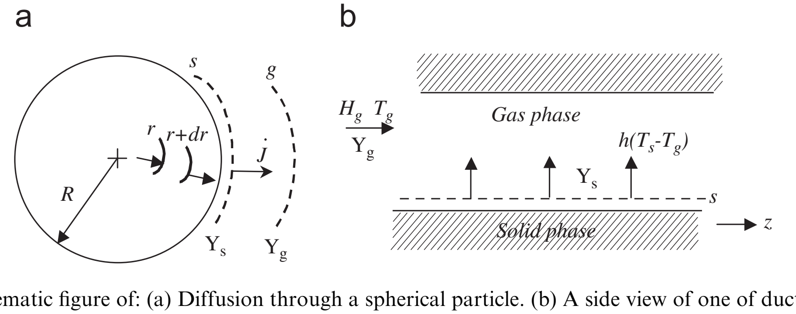


Fig. 13. Schematic figure of: (a) Diffusion through a spherical particle. (b) A side view of one of ducts for a PCP model [39].

diffusion within a desiccant particle is developed and included in PCP model to represent the moisture conservation in solid desiccant.

Pesaran and Mills [39,61] proposed a PCP model for simultaneous heat and mass transfer in a thin packed bed of silica gel particles. It believed that diffusion of moisture through the porous particle consists of Knudsen diffusion and surface diffusion. The spherical particle model and adsorption bed model are illustrated in Fig. 13.

The general form of moisture conservation equation for the spherical particle with radial symmetry was derived and given by:

$$\frac{\partial W}{\partial t} = \frac{1}{r^2}\frac{\partial}{\partial r}\left(D_e \cdot r^2 \cdot \frac{\partial W}{\partial r}\right), \tag{147}$$

where D_e is the total effective diffusivity which includes Knudsen diffusion and surface diffusion:

$$D_e = D_{\mathrm{S,eff}} + D_{k,\mathrm{eff}}\frac{g'(W)}{\rho_p}, \quad g'(W) = \rho_g\left(\frac{\partial Y}{\partial W}\right)_T. \tag{148}$$

For the thin beds, storage term $\partial Y_g/\partial t$ was negligible and moisture conservation equation in the air was

$$\dot{m}_g\frac{\partial Y_g}{\partial z} = K_y(Y_s - Y_g)(1 - Y_g)P. \tag{149}$$

Conservation of energy in gas-side was described by

$$c_{pg}\dot{m}_g\frac{\partial T_g}{\partial z} = -P[h + c_{pv} \cdot K_y(Y_s - Y_g)] \cdot (T_g - T_s), \tag{150}$$

where axial and radial conduction and the storage term $\partial T_g/\partial z$ have been neglected and the bed is assumed to be adiabatic.

Energy conservation in the solid desiccant yielded:

$$A\rho_m c_{pm}\frac{\partial T_s}{\partial t} = P[h(T_g - T_s) - q_{st}K_y(Y_s - Y_g)], \tag{151}$$

where subscript "m" represents the adsorption bed.

Eqs. (147) and (149) were linked by the equilibrium relation at the particle surface

$$Y_s(z,t) = [W(r = R, z, t), T_s(z,t), P_s]. \tag{152}$$

The boundary conditions and initial condition for Eq. (147) were

$$\left.\frac{\partial W}{\partial r}\right|_{r=0} = 0, \tag{153}$$

$$-\rho_{\mathrm{particle}}D\frac{\partial W}{\partial r}_{r=R} = K_y[Y_s(z,t) - Y_g(z,t)], \tag{154}$$

$$W(z, r, t = 0) = W_0. \tag{155}$$

The boundary condition for Eq. (150) was

$$T_g(z = 0, t) = T_{\mathrm{in}}. \tag{156}$$

While the initial condition for Eq. (151) was

$$T_s(z, t=0) = T_0. \tag{157}$$

Heat and mass transfer coefficients were obtained by experimental correlations [21]:

$$K_y = 1.70 m_a^{'}\,\mathrm{Re}^{-0.42}, \tag{158}$$

$$h = 1.60 m_a^{'}\,\mathrm{Re}^{-0.42} c_{pg}. \tag{159}$$

The properties for RD gel and ID gel were the same as Eqs. (36), (126)–(128), and specific heats of the gas and felt were

$$c_{pg} = 1884 Y_g + 1004(1 - Y_g), \tag{160}$$

$$c_{pm} = 4186 W_{\mathrm{avg}} + 921 \quad W_{\mathrm{avg}} = \int_0^{\mathrm{R}} 4\pi r^2 W \rho_P \,\mathrm{d}r/(4/3)\pi R^3 \rho_P. \tag{161}$$

The governing equations were put into dimensionless form and solved by finite difference method. Crank–Nicholson method was adopted for Eq. (147). Implicit Euler method was applied for Eq. (151). A fourth-order Runge–Kutta technique was used for Eqs. (149), (150). The transient results of this model were compared with the predictions of PGS model. It was proved that the simulated results getting from the new model agree better with the experimental data than those from PGS model for both ID gel and RD gel desiccant material.

Chant and Jeter [40] performed a steady state and transient analysis of rotary desiccant dehumidifier using a PCP model. The heat transfer equation and conservation equation in the desiccant side were similar to those of PGS model (Eqs. (77), (78), (81)), except for gas-side transfer coefficients h and K_y not compound transfer coefficients like h' and K_y' were adopted in PCP model. For mass transfer analysis, a parabolic concentration profile was assumed to exist in desiccant particle at all times, and for a spherical particle the profile was

$$W = a_1 + a_2(r/R)^2. \tag{162}$$

The moisture conservation equation for a spherical particle was

$$\frac{\partial W}{\partial t} = -\frac{3K_y}{\rho_{\mathrm{particle}} r}[Y_d(W_s, T_d) - Y_a], \tag{163}$$

where W_s is desiccant surface concentration which is derived using Eq. (162), Y_d stands for moist air equilibrium humidity ratio, they could be calculated by the following equation:

$$W_s = -\frac{K_y r_{\mathrm{particle}}}{5\rho_{\mathrm{particle}} D_e}[Y_d(W_s, T_d) - Y_a] + W, \tag{164}$$

$$Y_d = c_0 + c_1 W + c_2 H_d + c_3 Y_a. \tag{165}$$

[62] The enthalpy and equilibrium adsorption isotherm expressions were similar to Eqs. (97)–(98) and Eq. (17).

First the governing equations (Eqs. (77)–(78), (81), (163)) were associated with the inlet states of moist air for processing and regeneration as well as the desiccant bed initial state to construct transient model, which was used to study startup effects. Then periodic steady

state model was distinguished by applying the following periodic boundary conditions:

$$H_d(z, t = 0) = H_d(z, t = t_r), \tag{166}$$

$$W(z, t = 0) = W(z, t = t_r). \tag{167}$$

Transient model and periodic steady state model constituted the whole PCP model. The transient model was solved using Bulirsch–Stoer integrator method [63]. An implicit periodic steady-state solution with a linear adsorption isotherm (Eq. (165)) which utilizes a sparse matrix solving routine was developed to solve periodic steady-state model.

Compared with the transient experimental results of a fixed bed dehumidifier. It was found that the PCP model does not predict well in the initial adsorption period, which is due to the reason that the moisture concentration profile is not parabolic until later in the sorption period. But the simulation results become similar to that of the PGS model as time moves on. Also the periodic steady state of a desiccant wheel system predicted by this numerical model has shown good agreement with the testing data of practical desiccant wheel at low and medium rotation rates condition. The authors discussed the efficiency and flexibility of PCP model too. Their results indicated that the model only requires 1–3 min on a 25 MHz 80486DX PC for the cased considered. And since the widely used adsorbent property effective diffusivity D_e is used in mass transfer equation, it has the capability to simulate a variety of desiccant materials. Hence, PCP model is extremely efficient and an excellent tool for investigating alternative desiccant materials.

5. Empirical model

Beccali et al. [64] believed the models based on the detailed heat and mass transfer phenomena inside desiccant wheel are too complex. The solving process is complicated and time-consuming. Hence, in order to evaluate the performance of various kinds of rotary desiccant wheels available in the market, they analyzed the available measurements data from the manufacturer thoroughly and developed empirical model for evaluating the performance of silica gel desiccant wheel. It should be emphasized that the units of enthalpy, temperature and humidity ratio are KJ/kg, °C and g/kg, respectively, in the study. The derived correlations were expressed as

$$Y_{\text{out}}/T_{\text{out}} = (F_1 Y_{\text{in}}^2 + F_2 Y_{\text{in}} + F_3)T_{\text{in}} + (F_4 Y_{\text{in}}^2 + F_5 Y_{\text{in}} + F_6), \tag{168}$$

where F_i is a second-order polynomial of T_{reg} and can be expressed as follows:

$$i = (A_i T_{\text{reg}}^2 + B_i T_{\text{reg}} + C_i), \quad i = 1, \ldots, 6, \tag{169}$$

where A_i, B_i, C_i are second-order polynomials of X_{reg},

$$A_i, B_i, C_i = a_i Y_{\text{reg}}^2 + b_i Y_{\text{reg}} + c_i, \quad i = 1, \ldots, 6. \tag{170}$$

The equations were used to forecast process air outlet temperature T_{out} and absolute humidity Y_{out} as a function of the temperature and humidity ratio of the regeneration air (T_{reg} Y_{reg}) and of the inlet state of process air (T_{in} Y_{in}). There are 54 parameters (a_i b_i c_i) that related to outlet condition T_{out} and Y_{out} in the model, so the model is named as "Model 54". Model 54 was carried out to predict the performance of silica gel desiccant wheel (type -I). It was observed that the calculated values obtained using this model are very close to the measured values.

However, for a different type of desiccant material, a new group of 54 coefficients are needed, which is a tedious job for users. Then, further simplification were attempted to overcome the complexities of "Model 54". The new model was expressed by the parameters Φ (relative humidity) and H (enthalpy)

$$\Delta\Phi = (\Phi_{\text{in}} - \Phi_{\text{out}}) = a(\Phi_{\text{in}} - \Phi_{\text{reg}}) + b, \tag{171}$$

$$\Delta H = (H_{\text{in}} - H_{\text{out}}) = a'(H_{\text{reg}} - H_{\text{in}}) + b', \tag{172}$$

where the enthalpy is calculated by

$$H = \frac{(2501 + 1.85T)Y}{1000} + 1.006T \tag{173}$$

the calculation of relative humidity ratio is based on empirical relation developed by Beccali [65]

$$\Phi = (18.6715Y + 1.7976)\mathrm{e}^{-0.053T}. \tag{174}$$

The new relational expressions only have four variables a, b, a', b', much less than the variable numbers of "Model 54". Three different kinds of desiccant wheels were used to validate this model, two are based on silica gel and another one is on lithium chloride. The results showed that the simplified model reasonably predict the performance of all wheels.

The above two empirical models are valid only for the wheel running with identical air flux in process and regeneration side. By adding correction factors, Beccali [66] further modified the model which can be used to forecast the system with unequal process and regeneration air-flow volume. The modified model was verified for the three different kinds of desiccant wheels.

6. Conclusion

Various mathematical models have been proposed to assess the performance of desiccant wheel for different operating design conditions. Generally, the mathematical models are based on heat and mass transfer phenomena inside the system. They can be divided into two main categories in terms of gas-side resistance (GSR) model and gas and solid-side resistance (GSSR) model. Within the two categories, the models can be subdivided based on the dimensions and the methods to represent solid-side resistance (SSR). GSR model has two dimension types: one-dimensional and two-dimensional. GSSR model can be classified into three sub-categories: pseudo gas-side (PGS) model, gas and solid-side (GSS) model and parabolic concentration profile (PCP) model. Also, using the measurements data, several empirical models to evaluate the performance of desiccant wheel are reviewed in this paper.

In the GSR model, heat and mass transfer within solid desiccant is not taken into account. The governing equations have relatively simple form with lower accuracy. PGS model adopts the lumped heat and mass transfer coefficients to represent the overall heat and mass transfer from the air stream to desiccant material. In theses models, convective heat and mass transfer coefficients are empirically degraded to account for both gas-side and solid-side resistances. Therefore, though its form is basically the same as GSR model, the accuracy is improved. The more practical model known as GSS model adds second-order heat and mass transfer diffusional terms directly into the governing equations. It is

more related to the actual process occurred in the desiccant wheel and the effect of SSRs can be well explained. The precision of this model is thus greatly improved. PGS model consumes less computational time but has lower flexibility and accuracy compared to GSS model. PCP model which assumes an analytically convection concentration profile within the desiccant particle appears to be a good compromise between fundamental principles, accuracy and computational speed. It is an excellent tool for performing seasonal simulations or repetitive design simulation particularly when alternative materials are investigated.

It can be seen that boundary conditions in Mode I are widely used in all the models whenever possible. Mode II and III boundary conditions are usually utilized in GSSR model. Other auxiliary relations such as heat of sorption and equilibrium isothermal have to be obtained to complete the mathematical model.

Due to the complex nature of the partial differential equations, it is necessary to solve the mathematical model using numerical methods. Finite difference method is recognized as the most accurate and most universal solution technique. Though other methods such as finite volume method [7,38], analogy method [31] and wave analysis method [33,57] are also used.

Beside, model validation is an important step in model development since it offers the possibility of comparing simulation results with actual system behavior. Experiments are mostly used to validate the mathematical model. Beside, compared with the previous numerical results is also a good validation method.

Though a large amount of works have been conducted on modeling and analyzing desiccant wheel, further efforts are still needed:

(i) To take account of the pressure and velocity loss through the channel.
(ii) To study the influence of variable thermophysical physical properties of moist air and desiccant materials which are taken as constant in almost all existing models.
(iii) To improve the accuracy of the model based on diffusion mechanism, since by now, there still no uniform theory exists.
(iv) To construct a simulation package of the whole desiccant air-conditioning system by combining the model of the wheel and other components in the system. Using object-oriented languages, Chau and Worek [67] simulated an open-cycle desiccant cooling system operating in the recirculation mode. As presented in the paper, the simulation package is ongoing and in the near future it is hoped that a graphical user interface can be applied in it (Tables 2 and 3).

Acknowledgements

We are deeply grateful to the financial support of both the Shanghai Expo special project (No: 2005B A908B 07 05dz 05807), and the Shanghai Rising-Star Program (No: 05qmx1437).

References

[1] Klein H, Klein SA, Michell JW. Analysis of regenerative enthalpy exchangers. Int J Heat Mass Transfer 1990;33(4):735–44.

[2] San J-Y. Heat and mass transfer in a two-dimensional cross-flow regenerator with a solid conduction effect. Int J Heat Mass Transfer 1993;36(3):633–43.
[3] Majumdar P, Worek WM. Combined heat and mass transfer in a porous adsorbent. Energy 1989;14(3):161–75.
[4] Barlow RS. An analysis of the adsorption process and of desiccant cooling system—A pseudo-steady-state model for coupled heat and mass transfer. Solar Energy Research Institute, Golden, Colo1982; SERI/TR-631-1330.
[5] Schultz KJ, Mitchell JW. Comparison of the DESSIM model with a finite difference solution for rotary desiccant dehumidifiers. ASME J Solar Energy Eng 1989;111(4):286–91.
[6] Zhang XJ. Study on dehumidification performance of silica gel-haloid composite desiccant wheel. Ph.D Thesis, Shanghai Jiao Tong University, 2004.7 [in Chinese].
[7] Simonson CJ, Besant RW. Heat and moisture transfer in desiccant coated rotary energy exchangers: part I: Numerical model. Int J HVAC R Res 1997;3(4):325–50.
[8] Yu JD, Luo G, Zhang HF. Mathematical model of rotary desiccant wheel and the code RDEH. Tai Yang Neng Xue Bao/ACTA ENERGIAE SOLARIS SINICA 1994.7;15(3):209–17 [in Chinese].
[9] Jurinak JJ, Mitchell JW. Effect of matrix properties on the performance of a counterflow rotary dehumidifier. ASME J Heat Transfer 1984;106(3):638–45.
[10] Charoensupaya D, Worek WM. Effect of adsorbent heat and mass transfer resistances on performance of an open cycle adiabatic desiccant cooling system. Heat Recovery System and CHP 1988;8(6):537–48.
[11] Banks PJ. Prediction of heat and mass regenerator performance using nonlinear analogy method: Part1-Basis. J Heat Transfer 1985;107(1):222–9.
[12] Banks PJ. Prediction of heat and mass regenerator performance using nonlinear analogy method: Part2-Comparision of Methods. J Heat Transfer 1985;107(1):230–7.
[13] Charoensupaya D, Worek WM. Parametric study of an open-cycle adiabatic, solid, desiccant cooling system. Energy 1988;13(9):739–47.
[14] Zheng W, Worek WM. Numerical simulation of combined heat and mass transfer processes in a rotary dehumidifier. Numer Heat Transfer, Part A: Appl 1993;23(2):211–32.
[15] Brandemuehl MJ. Analysis of heat and mass transfer regenerators with time varying or spatially nonuniform inlet conditions. Ph.D Thesis, Department of mechanical engineering. University of Wisconsin, 1982.
[16] Zheng W, Worek WM, Novosel D. Control and optimization of rotational speeds for rotary dehumidifiers. ASHRAE Trans 1993;99(Part 1):825–33.
[17] Zheng W, Worek WM, Novesel D. Performance optimization of rotary dehumidifiers. ASME J Solar Energy Eng 1995;117:40–4.
[18] Zheng W, Worek WM, Novosel D. Effect of operating conditions on optimal performance of rotary dehumidifiers. Journal of Energy Res Technol, Trans ASME 1995;117(1):62–6.
[19] Zhang XJ, Dai YJ, Wang RZ. Simulation study of heat and mass transfer in a honey combed rotary desiccant dehumidifier. Proceedings of the 2003 fourth international symposium on heating, ventilating and air conditioning; p. 805–16.
[20] Zhang XJ, Dai YJ. A simulation study of heat and mass transfer in a honeycombed rotary desiccant dehumidifier. Appl Thermal Eng 2003;23(8):989–1003.
[21] Pesaran AA. Air dehumidification in packed silica gel beds. M.S. Thesis, School of engineering and applied science. University of California Los Angeles, 1980.
[22] Sherony DF, Solbrig CW. Analytical investigation of heat or mass transfer and friction factors in a corrugated duct heat or mass exchanger. Int J Heat Mass Transfer 1970;13:145–59.
[23] Shah RK, London AL. In: Irvine TF, Hartnett, editors. Advances in Heat Transfer: Laminar flow forced convection in ducts: a source book for compact heat exchanger analytical data. New York: Academic Press; 1978.
[24] Patankar SV. Numerical heat transfer and fluid flow. NewYork: Hemisphere; 1980.
[25] Simonson CJ, Besant RW. Heat and moisture transfer in desiccant coated rotary energy exchangers: part II: Validation and sensitivity studies. Int J HVAC R Res 1997;3(4):351–68.
[26] Mihajlo NG, William MW. Influence of elevated pressure on sorption in desiccant wheels. Numer Heat Transfer part A 2004;45:869–86.
[27] Zhong JH. Experimental study on rotary wheel fabricated with ceramic coated with compound desiccant. M.S. Thesis, Shanghai Jiao Tong University, 2005.1 (in Chinese).
[28] Simonson CJ, Besant RW. Heat and moisture transfer in energy wheels during sorption, condensation, and frosting conditions. ASME J Heat Transfer 1998;120(3):699–708.

[29] Simonson CJ, Besant RW. Energy wheel effectiveness: part I development of dimensionless groups. Int J Heat Mass Transfer 1999;42(12):2161–70.

[30] Jeong J-W, Stanley AM. Practical thermal performance correlations for molecular sieve silica gel loaded enthalpy wheels. Appl Thermal Eng 2005;25(5–6):719–40.

[31] Feng Q, Yu JD, Zhang HF. Similarity analysis and computation of a rotary solid desiccant dehumidifier. Tai Yang Neng Xue Bao 1994(4);15(2):103–24 [in Chinese].

[32] Holmberg RB. Combined heat and mass transfer in regenerators with hygroscopic materials. ASME J Heat Transfer 1979;101:205–10.

[33] Van den Bulck E, Mitchell JW, Klein SA. Design theory for rotary heat and mass exchangers I: Wave analysis of rotary heat and mass exchangers with infinite transfer coefficients. Int J Heat Mass Transfer 1985; 28(8):1575–86.

[34] Elsayed MM, Chamkha AJ. Analysis and performance of radial flow rotary desiccant dehumidifiers. J Solar Energy Eng 1997;119(1):35–43.

[35] San JY, Hsiau SC. Effect of axial solid heat conduction and mass diffusion in a rotary heat and mass regenerator. Int J Heat Mass Transfer 1993;36(8):2051–9.

[36] Yu JD, Luo G, Zhang HF. New mathematical model of a rotary desiccant wheel and the program of RDCS. Tai Yang Neng Xue Bao 1995;16(4):368–78 [in Chinese].

[37] Zhang LZ, Niu JL. Performance comparisons of desiccant wheels for air dehumidification and enthalpy recovery. Appl Thermal Eng 2002;22(12):1347–67.

[38] Sphaier LA, Worek WM. Analysis of heat and mass transfer in porous sorbents used in rotary regenerators. Int J Heat Mass Transfer 2004;47(14–16):3415–30.

[39] Pesaran AA, Mills AF. Moisture transport in silica gel packed beds. I—theoretical study. Int J Heat Mass Transfer 1987;30(6):1037–49.

[40] Chant EE, Jeler SM. On the use of the parabolic concentration profile assumption for a rotary desiccant dehumidifier. J Solar Energy Eng 1995;117(1):45–50.

[41] Hougen OA, Marshall WR. Adsorption from a fluid stream flowing through a stationary granular bed. Chem Eng Prog 1947;43(4):197–208.

[42] Ahlberg JE. Rates of water vapor adsorption for air by silica gel. Ind Eng Chem 1939;31:988–92.

[43] Maclaine-Cross IL. A theory of combined heat and mass transfer in regenerators. Ph.D thesis, Department of mechanical engineering. Monash University, Clayton,Vic, Australia, 1974.

[44] Cejudo JM, Moreno R, Carrillo A. Physical and neural network models of a silica-gel desiccant wheel. Energy and Buildings 2002;34(8):837–44.

[45] Jurinak JJ. Open cycle solid desiccant cooling—component models and system simulation. PhD thesis, Mechanical Engineering Department; University of Wisconsin, Madison, 1982.

[46] Van Den Bulck E, Mitchell JW, Klein SA. Design theory for rotary heat and mass exchangers—II. Effectiveness-number-of-transfer-units method for rotary heat and mass exchangers. Int J Heat Mass Transfer 1985;28(8):1587–95.

[47] Van den Bulck E, Mitchell JW, Klein SA. The use of dehumidifiers in desiccant cooling and dehumidification systems. J Heat Transfer 1986;108(3):684–92.

[48] Rau JJ, Klein SA, Mitchell JW. Characteristics of lithium chloride in rotary heat and mass exchangers. Int J Heat Mass Transfer 1991;34(11):2703–11.

[49] Pla-Barby PE, Vliet GC, Pauton RL. 1978 Performance of rotary bed silica gel solid desiccant dryers. ASME Paper No78-HT-36.

[50] Clark JE, Mills AF, Buchberg H. Design and testing of thin adiabatic desiccant beds for solar air conditioning applications. J Solar Energy Eng 1981;103:89–91.

[51] Mei VC, Lavan Z. Performance of cross-cooled desiccant dehumidifiers. ASME J Solar Energy Eng 1983; 105(3):300–4.

[52] Ghezelayagh H, Gidaspow D. Micro-Macropore model for sorption of water on silica gel in a dehumidifier. Chem Eng Sci 1982;37(8):1181–97.

[53] Raghavan V. Diffusion and adsorption of moisture in desiccant sheets. Ph.D. Thesis, Illinois Institute of Technology; 1982.

[54] Zhang HF, Yu JD. Research and development of the key components for desiccant cooling system. Renewable Energy 1996;9(1–4):653–6.

[55] Pla-Barby FE, Vliet GC. Rotary bed solar drying: An analytical and experimental investigation. Proceeding of the joint ASME/AICHE 18th national heat transfer conference. San Diego, CA, August 6–8, 1979:7–8.

[56] Colier RK, Cohen BM, Slosber RB. Desiccant properties and their effects on the performance of desiccant cooling systems. ASHRAE, Inc., IS N 0-910110-90-5, 1992.
[57] Dai YJ, Wang RZ, Zhang HF. Parameter analysis to improve rotary desiccant dehumidification using a mathematical model. Int J Thermal Sci 2001;40(4):400–8.
[58] Gao Z, Mei VC, Tomlinson JJ. Theoretical analysis of dehumidification process in a desiccant wheel. Heat and Mass Transfer 2005;41(11):1033–42.
[59] Samarskii AA, Vabishchevich PN. Computational heat transfer. New York: Wiley; 1995.
[60] Niu JL, Zhang LZ. Effects of wall thickness on the heat and moisture transfers in desiccant wheels for air dehumidification and enthalpy recovery. Int Commun Heat Mass Transfer 2002;29(2):255–68.
[61] Pesaran AA, Mills AF. Moisture transport in silica gel packed beds—II. Experimental study. Int J Heat Mass Transfer 1987;30(6):1051–60.
[62] ASHRAE. Fundamentals. ASHRAE: Atlanta. GA; 1985.
[63] Bulirsch R, Stoer J. Numerical treatment of ordinary differential equations by extrapolation method. Numer Math 1966;8:1–13.
[64] Beccali M, Butera F, Guanella R, Adhikari RS. Simplified models for the performance evaluation of desiccant wheel dehumidification. Int J Energy Res 2003;27(1):17–29.
[65] Beccali M, Butera F, Guanella R, Adhikari RS. Performance evaluation of rotary desiccant wheels. Proceeding of world renewable energy congress (WREC)-VI, Cologne, Germany, July 2002.
[66] Beccali M, Adhikari RS, Butera F, Franzitta V. Short communication. Update on desiccant wheel model. Int J Energy Res 2004;28(12):1043–9.
[67] Chau CK, Worek WM. Interactive simulation tools for open-cycle desiccant cooling systems. ASHRAE Trans 1995;1:725–34.